JOC The Journal of Organic Chemistry

Article

pubs.acs.org/joc

Phenothiazine-Bridged Cyclic Porphyrin Dimers as High-Affinity Hosts for Fullerenes and Linear Array of C_{60} in Self-Assembled Porphyrin Nanotube

Ken-ichi Sakaguchi,[†] Takuya Kamimura,[†] Hidemitsu Uno,[‡] Shigeki Mori,[§] Shuwa Ozako,[†] Hirofumi Nobukuni,[†] Masatoshi Ishida,[†] and Fumito Tani*[,†]

[†]Institute for Materials Chemistry and Engineering, Kyushu University, 6-10-1 Hakozaki, Higashi-ku, Fukuoka 812-8581, Japan

[‡]Graduate School of Science and Engineering, Ehime University, Bunkyo-cho, Matsuyama, Ehime 790-8577, Japan

[§]Integrated Center for Sciences, Ehime University, Bunkyo-cho, Matsuyama, Ehime 790-8577, Japan

Supporting Information

ABSTRACT: Free-bases and a nickel(II) complex of phenothiazine-bridged cyclic porphyrin dimers bearing self-assembling 4-pyridyl groups (M_2-Ptz-$CPD_{py}(OC_n)$; M = H_2 or Ni, OC_n = OC_6 or OC_3) at opposite *meso*-positions have been prepared as host molecules for fullerenes. The free-base dimer (H_4-Ptz-$CPD_{py}(OC_6)$) includes fullerenes with remarkably high association constants such as $3.9 \pm 0.7 \times 10^6$ M^{-1} for C_{60} and $7.4 \pm 0.8 \times 10^7$ M^{-1} for C_{70} in toluene. This C_{60} affinity is the highest value ever among reported receptors composed of free-base porphyrins. The nickel dimer (Ni_2-Ptz-$CPD_{py}(OC_6)$) also shows high affinities for C_{60} ($1.3 \pm 0.2 \times 10^6$ M^{-1}) and C_{70} (over 10^7 M^{-1}). In the crystal structure of the inclusion complex of C_{60} within H_4-Ptz-$CPD_{py}(OC_3)$, the C_{60} molecule is located just above the centers of the porphyrins. The two porphyrin planes are almost parallel to each other and the center-to-center distance (12.454 Å) is close to the optimal separation (~12.5 Å) for C_{60} inclusion. The cyclic porphyrin dimer forms a nanotube through its self-assembly induced by C−H···N hydrogen bonds between porphyrin β-CH groups and pyridyl nitrogens as well as $\pi-\pi$ interactions of the pyridyl groups. The C_{60} molecules are linearly arranged in the inner channel of this nanotube.

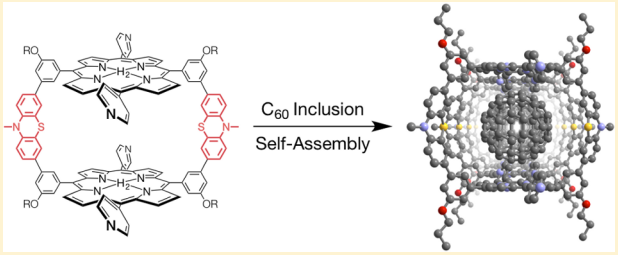

INTRODUCTION

Fullerenes have been widely used as electron acceptors, owing to their favorable reduction potentials and small reorganization energy in electron transfer reactions.[1] They are promising materials for organic photovoltaics (OPV) and molecular electronics.[1] For these applications, it is essential to prepare well-ordered arrangements of fullerenes. However, the control of arrangements of fullerenes has not been fully developed, especially for unmodified fullerenes, because pristine fullerenes are composed of only sp^2-carbon atoms and have neither polarity nor functional group. Our strategy for solving this problem is to use a host molecule having the following two functions: (i) efficient complexation with fullerenes; (ii) ability to form a self-assembled array of a predictable structure. The resulting host−guest complex affords a desired arrangement of fullerene through the self-assembly of the host molecule (Scheme 1). The molecular design of a host for fullerenes is the key in this supramolecular approach.[2] From this viewpoint, porphyrin derivatives are especially useful building components for host molecules fulfilling the above two requirements.[3] It has been known that strong $\pi-\pi$ interactions between the curved π-surfaces of fullerenes and the flat π-planes of porphyrins exist in both solution and crystalline state. A number of host molecules composed of multiporphyrinic moieties have been reported to give stable inclusion complexes with fullerenes so far.[4] In addition, there have been a wealth of chemical modifications for porphyrin derivatives, and various self-assembling functional groups have been introduced into porphyrin frameworks to obtain a variety of assembled structures.[5]

Meanwhile, porphyrin derivatives have unique light-harvesting properties, for example, strong absorption bands in the visible region and electron-donating abilities of their photoexcited states.[6] Large numbers of the donor−acceptor combinations of porphyrins and fullerenes have been studied as functional mimics of the reaction center for charge separation in natural photosynthesis.[7] Long-lived photoinduced charge separations with high quantum yields have been reported by the optimization of the geometries and energy levels of these chromophores.[8] Porphyrins and fullerenes have been used as donors and acceptors also for organic photovoltaic (OPV) devices.[9] The mechanism of the conversion from photons to photocurrent in OPV is composed of three important processes; light harvesting, charge separation and charge transport. It has been revealed that a well-ordered

Received: January 8, 2014
Published: March 5, 2014

dx.doi.org/10.1021/jo500034f | J. Org. Chem. 2014, 79, 2980−2992

Scheme 1. Formation of Linear Array of Fullerene in Self-Assembled Porphyrin Nanotube

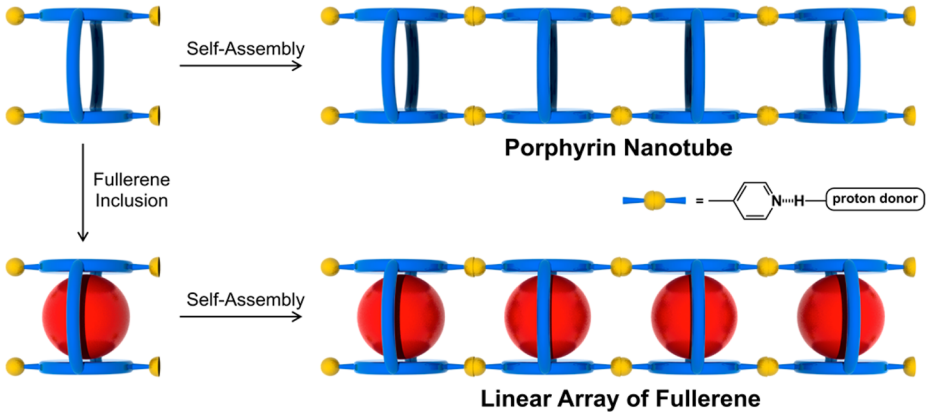

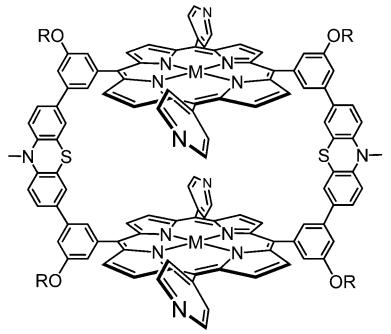

H_4-Ptz-$CDP_{Py}(OC_6)$: M = H_2, OR = OC_6H_{13}
H_4-Ptz-$CDP_{Py}(OC_3)$: M = H_2, OR = OC_3H_7
Ni_2-Ptz-$CDP_{Py}(OC_6)$: M = Ni, OR = OC_6H_{13}

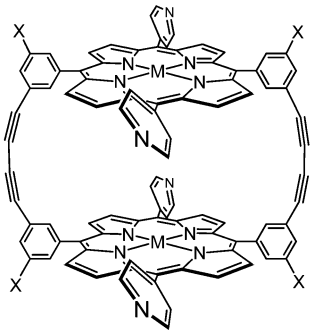

H_4-C_4-$CDP_{Py}(H)$: M = H_2, X = H
Ni_2-C_4-$CDP_{Py}(H)$: M = Ni, X = H
H_4-C_4-$CDP_{Py}(OC_6)$: M = H_2, X = OC_6H_{13}
Ni_2-C_4-$CDP_{Py}(OC_6)$: M = Ni, X = OC_6H_{13}

Figure 1. Chemical structures of cyclic porphyrin dimers.

bicontinuous donor−acceptor array in the active layer is an ideal structure to realize the above processes and is effective for the improvement of the power conversion efficiency in OPV.[10] Therefore, we have focused our attention on the creation of a linear arrangement of fullerene inside a self-assembled nanotube of a porphyrin host, the array of which is expected to perform photoinduced charge separation and smooth vectorial charge transport.

For preparing supramolecular organic nanotubes, one of the most straightforward methods is to introduce self-assembling groups into rigid cyclic molecules and align them through noncovalent interactions (Scheme 1).[11] Along this method, we have prepared the nickel complex and free-base of the butadiyne-linked cyclic porphyrin dimer bearing self-assembling 4-pyridyl groups at the trans *meso*-positions (Ni_2-C_4-$CPD_{Py}(H)$ and H_4-C_4-$CPD_{Py}(H)$ in Figure 1).[12] Both porphyrin dimers afford stable inclusion complexes with fullerenes such as C_{60},[12a−c] $Li^+@C_{60}$,[12f] PCBM ([6,6]-phenyl-C_{61}-butyric acid methyl ester),[12e] and C_{70}.[12d] In the crystal structure of the inclusion complex of the nickel dimer and C_{60} (C_{60}⊂Ni_2-C_4-$CPD_{Py}(H)$), C_{60} molecules are linearly arranged in the inner channel of the self-assembled porphyrin nanotube.[12a] The self-assembly is induced by two kinds of noncovalent interactions: (i) nonclassical C−H···N hydrogen bonds between porphyrin *β*-CH groups and pyridyl nitrogen atoms, (ii) *π*−*π* interactions of the *meso*-pyridyl groups. This crystal shows anisotropic high electron mobility ($\Sigma\mu$ = 0.72 $cm^2\ V^{-1}\ s^{-1}$) along with the linear arrangement of C_{60}.[12b] However, the expected charge-separated state of C_{60}⊂Ni_2-C_4-$CPD_{Py}(H)$ was not detected in the time-resolved transient absorption spectra, because the singlet excited state of the nickel porphyrin transforms very rapidly to the triplet excited state via the intersystem crossing, then the low-energy triplet excited state of C_{60} ($^3C_{60}$*) arises as a consequence of energy transfer. The estimated energy level of charge-separated state (1.98 eV) is much higher than that of $^3C_{60}$* (1.57 eV).[13] On the other hand, the inclusion complex of the free-base dimer and C_{60} (C_{60}⊂H_4-C_4-$CPD_{Py}(H)$) contains a zigzag array of C_{60} molecules through van der Waals contact with each other and also exhibits a high charge mobility ($\Sigma\mu$ = 0.13−0.16 $cm^2\ V^{-1}\ s^{-1}$) along the C_{60} array in the crystalline state.[12c] Further, it affords a photoinduced charge-separated state via electron transfer from the porphyrin to C_{60} due to the lower oxidation potential and the slower intersystem crossing of the free-base porphyrin than those of the nickel complex.

As mentioned above, C_{60}⊂Ni_2-C_4-$CPD_{Py}(H)$ gives the self-assembled nanotube including the linear array of C_{60}, whereas C_{60}⊂H_4-C_4-$CPD_{Py}(H)$ is unable to form a nanotube structure. The reason for the difference of these assembled structures is as following. In the crystal structure of C_{60}⊂Ni_2-C_4-$CPD_{Py}(H)$, the center-to-center distance of the two porphyrins is 12.596(2) Å, being enough to accommodate C_{60} with the pseudoparallel conformation of the two porphyrins (Scheme 2). In contrast, in the case of C_{60}⊂H_4-C_4-$CPD_{Py}(H)$, the porphyrin dimer takes a clamshell conformation due to the shorter center-to-center distance (11.126 Å). Only the pseudoparallel conformation provides the self-assembled nano-

dx.doi.org/10.1021/jo500034f | J. Org. Chem. 2014, 79, 2980−2992

Scheme 2. Schematic Illustrations of the Crystal Structures of the C_{60} Inclusion Complexes of Butadiyn-Bridged Cyclic Porphyrin Dimers

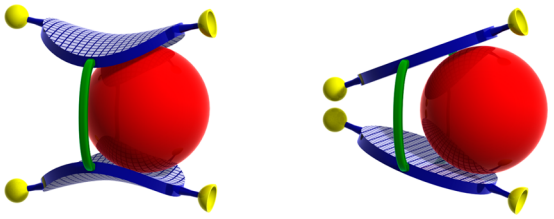

C_{60}⊂Ni_2-C_4-CPD_{Py}(H) C_{60}⊂H_4-C_4-CPD_{Py}(H)

tube through the C−H···N_{Py} hydrogen bonds and the $\pi-\pi$ interactions of the pyridyl groups. These noncovalent interactions are impossible for the clamshell conformation. Although Ni_2-C_4-CPD_{Py}(H) and H_4-C_4-CPD_{Py}(H) have the same butadiynyl linkages, the nickel porphyrins have ruffled distortions to achieve the longer center-to-center distance, while the higher planarity of the free-base porphyrins leads to the shorter distance.

On the basis of these results, we have intended to design a new cyclic porphyrin dimer as a host molecule for fullerenes, which can satisfy the following two requirements: (i) to form a self-assembled nanotube structure including a linear array of C_{60},[14] (ii) to give a photoinduced charge-separated state between the porphyrin host and fullerenes, that is, the use of a free-base porphyrin dimer rather than the corresponding nickel complex. For the self-assembled nanotube structure of a C_{60} inclusion complex, a new cyclic dimer should have *meso*-pyridyl groups as well as rigid longer linkages, which can keep its center-to-center distance at ∼12.5 Å even for a free-base dimer to realize a pseudoparallel conformation upon C_{60} inclusion. We herein report the synthesis of free bases and a nickel complex of phenothiazine-bridged cyclic porphyrin dimers and characterization of their inclusion complexes with fullerene C_{60} and C_{70} by spectroscopic and X-ray crystallographic analysis.

RESULTS AND DISCUSSION

Molecular Design and Synthesis of Phenothiazine-Bridged Porphyrin Dimers. In order to construct self-assembled porphyrin nanotubes including a linear array of C_{60},

Scheme 3

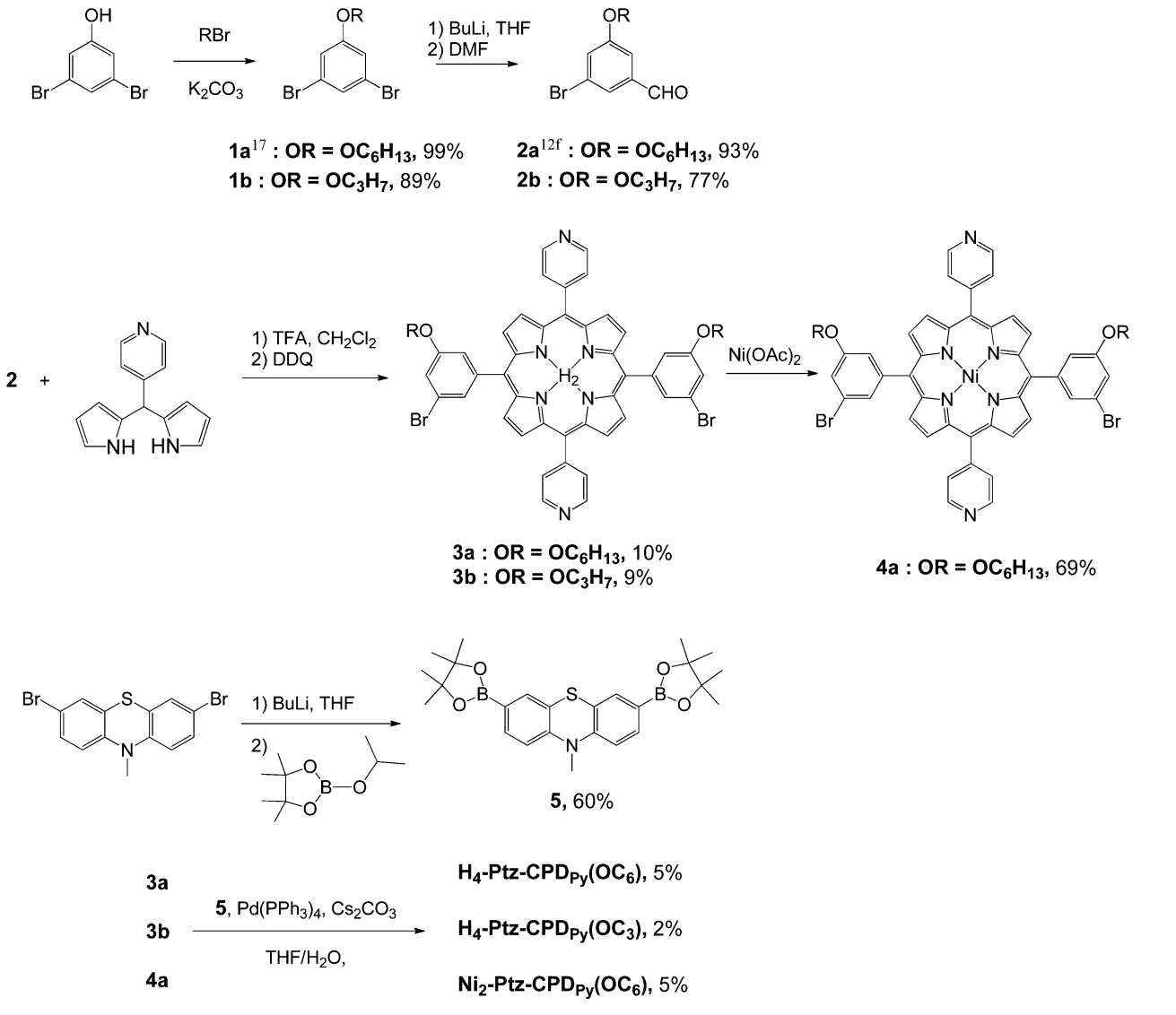

dx.doi.org/10.1021/jo500034f | J. Org. Chem. 2014, 79, 2980−2992

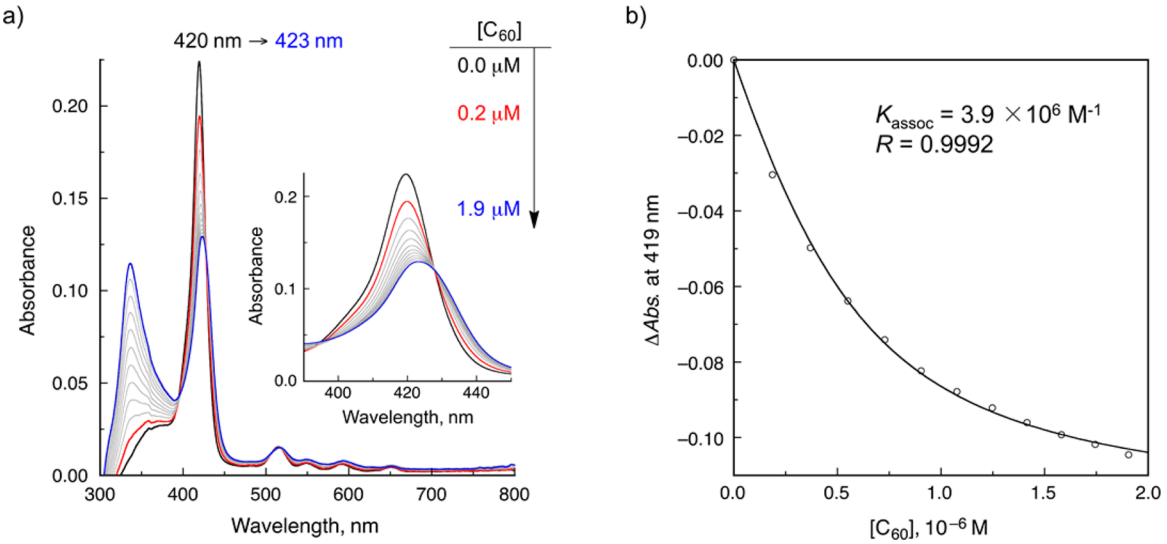

Figure 2. (a) UV−vis absorption spectral changes of H_4-Ptz-$CPD_{Py}(OC_6)$ in the course of titration with C_{60} in toluene at 25 °C. [H_4-Ptz-$CPD_{Py}(OC_6)$] = 5.0×10^{-7} M. The inset shows the magnified Soret band region. (b) Plot of the changes in the UV−vis absorbance (ΔAbs) at 419 nm versus the concentration of C_{60}. The curve was fitted by using eq 1

we have designed new cyclic porphyrin dimers which have 4-pyridyl groups at the *trans-meso*-positions and phenothiazine linkers (M_2-Ptz-$CPD_{Py}(OC_n)$; M = H_2 or Ni, OC_n = OC_6 or OC_3 in Figure 1). Phenothiazine derivative has a rigid aromatic framework wherein three six-membered rings are linearly fused. However, the butterfly structure of phenothiazine has some extent of flexibility with the change of dihedral angle between two benzene rings from ∼140° up to ∼160°.[15] The cavity size of the phenothiazine-bridged dimers can thus be adapted for inclusion of a fullerene molecule through the alteration of the dihedral angles. Based on the DFT (M06-2X/6-31G(d,p))-optimized[16] model structure of the inclusion complex of a phenothiazine-bridged free-base dimer (H_4-Ptz-$CPD_{Py}(H)$) and C_{60}, the two porphyrins are in a pseudoparallel conformation, and the center-to-center distance is estimated to be 12.2 Å (Figure S1 and Table S1 in Supporting Information [SI]). In the calculation, the outside alkoxyl groups are omitted to simplify the structure. The calculated center-to-center distance is close to the optimal value (∼12.5 Å)[4m] for C_{60} inclusion by porphyrin dimers such as our C_{60}⊂Ni_2-C_4-$CPD_{Py}(H)$ (12.596(2) Å)[12a] and the C_{60} inclusion complex of the cyclic zinc porphyrin dimer by Aida et al. (12.352(1) Å).[4d]

In order to improve the low solubility of the pyridyl-substituted porphyrins, we have introduced four alkoxyl chains (e.g., OC_6H_{13} or OC_3H_7) onto the *meso*-phenyl groups. H_4-Ptz-$CPD_{Py}(OC_3)$ has lower solubility than H_4-Ptz-$CPD_{Py}(OC_6)$ but is more suitable for making single crystals for X-ray crystallographic analysis. The free-base and nickel complex of the hexyloxy-substituted dimer are mainly employed for the spectroscopic investigation of the inclusion in solution.

Although the free base of the new cyclic porphyrin dimer is the main target compound in this study, we additionally synthesized the nickel complex for the comparative evaluation of the free base derivative. The reasons for the choice of the nickel complex are as follows. (a) A nickel(II) complex of porphyrin is electronically neutral. When a metal complex is not electronically neutral, the presence of the counterion sometimes affects the assembled structure of the metal complex. (b) A nickel(II) complex of porphyrin is air stable. (c) A nickel(II) complex of porphyrin is diamagnetic and allows usual ^{1}H- and ^{13}C NMR analysis of the dimer and its fullerene inclusion complexes. (d) A low-spin nickel(II) complex of porphyrin favors four-coordinate geometry to avoid the axial ligation of the *meso*-pyridyl groups. For example as another metal complex adopting five- or six-coordinate geometry, the zinc complex of these dimers is hardly soluble in organic solvents except pyridine due to the intermolecular axial coordination of the *meso*-pyridyl groups. While the zinc complex of the dimer fulfills the requirements (a−c), it is not employed in this study because of the last reason, (d).

The new dimers have been prepared by palladium-catalyzed Suzuki−Miyaura coupling reactions of the dibrominated porphyrin monomers and the bis-borylated phenothiazine derivative (Scheme 3). The porphyrin monomers (**3**) were obtained by using TFA-catalyzed [2 + 2]-type condensation reaction of *meso*-pyridyl-dipyrromethane[18] and 3-bromo-5-alkoxylbenzaldehyde[12f] (**2**) and subsequent DDQ (2,3-dichloro-5,6-dicyano-*p*-benzoquinone) oxidation in ∼10% yield.[19] The nickel(II) porphyrinato complex (**4a**) was synthesized by refluxing (**3a**) with nickel(II) acetate (10 equiv) in $CHCl_3$/MeOH solution. The bis-pinacolate boronic ester of phenothiazine (**5**) was obtained by borylation of the corresponding dibrominated phenothiazine derivative.[20] Finally, the cyclic porphyrin dimer, H_4-Ptz-$CPD_{Py}(OC_6)$, was synthesized by Suzuki−Miyaura coupling reaction of the free-base porphyrin monomer (**3a**) and phenothiazine derivative (**5**) under refluxing with 40 mol % $Pd(PPh_3)_4$ and Cs_2CO_3 (10 equiv) in THF/H_2O (10/1) under N_2 atmosphere for 48 h. The crude product was purified by gel permeation chromatography (GPC) to obtain a fraction containing the desired cyclic dimer. After recrystallization from $CHCl_3$/MeOH, the pure form of H_4-Ptz-$CPD_{Py}(OC_6)$ was isolated in 5% yield. It was found that the use of aqueous THF as a reaction media is critical to obtain the desired product in this palladium-catalyzed reaction. Different solvent systems such as toluene/DMF (10/1) resulted in considerable decrease of the product yields (1−2%). H_4-Ptz-$CPD_{Py}(OC_3)$ and Ni_2-Ptz-$CPD_{Py}(OC_6)$ were also prepared under the same reaction condition as H_4-Ptz-$CPD_{Py}(OC_6)$ in the similar yields. These isolated cyclic

dx.doi.org/10.1021/jo500034f | J. Org. Chem. 2014, 79, 2980−2992

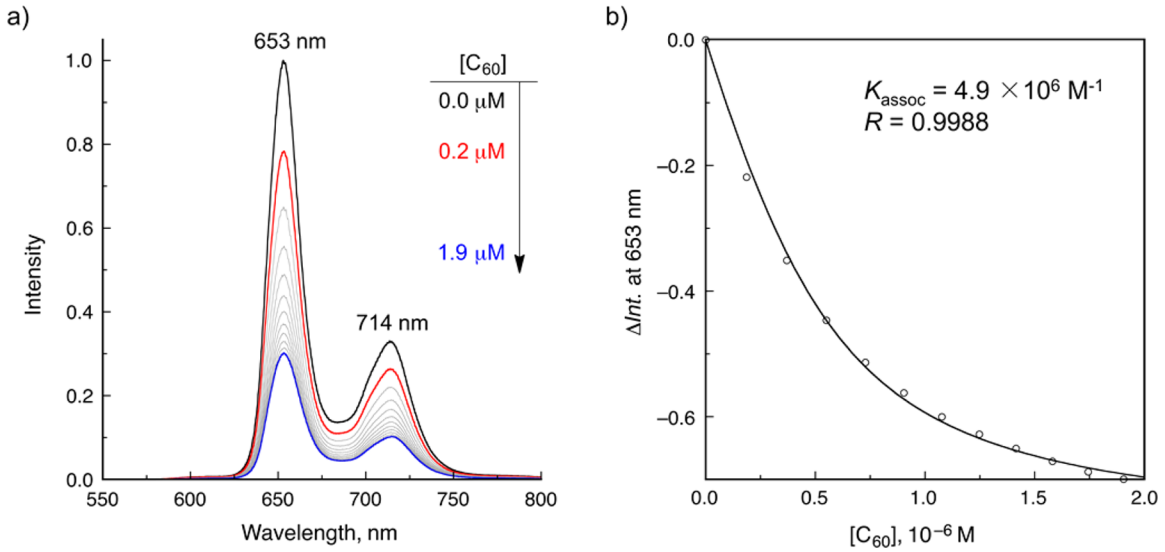

Figure 3. (a) Fluorescence spectral changes of H_4-Ptz-$CPD_{Py}(OC_6)$ in the course of titration with C_{60} in toluene at 25 °C excited at 426 nm. [H_4-Ptz-$CPD_{Py}(OC_6)$] = 5.0×10^{-7} M. (b) Plot of the changes in the fluorescence intensity (ΔInt) at 653 nm versus the concentration of C_{60}. The curve was fitted by using eq 3

porphyrin dimers were fully characterized by ^{1}H NMR, high resolution FAB mass, and IR and UV−vis absorption spectroscopies (see Experimental Section and SI).

Inclusion of C_{60} and C_{70} within CPD_{Py} in Solution. We have investigated the inclusion behaviors of C_{60} as well as C_{70} within the cyclic porphyrin dimers in solution by various methods such as UV−vis absorption, fluorescence, ESI-MS, and ^{13}C NMR spectroscopies.

Herein, A and X are $[CPD_{Py}]_0$ and $[fullerene]_0$, respectively; $\Delta\varepsilon$ is the difference of absorption coefficient between CPD_{Py} and its inclusion complex; ε_{70} is the absorption coefficient of free C_{70} at the examined wavelength. K_{assoc} and $\Delta\varepsilon$ were treated as fitting parameters. The association constants higher than 10^7 M^{-1} could not be determined precisely by UV−vis spectroscopy.

Fullerene inclusion behaviors of the free-base dimers were also investigated by fluorescence spectroscopy. When the free-base dimers are photoexcited in toluene, the fluorescence is observed with λ_{max} = ∼650 and 715 nm as shown in Figure 3, S5 and S6 in SI. The addition of fullerenes to the free-base dimers causes a prominent decrease of the fluorescence intensity. As control experiments, the fluorescence spectra of the free-base monomer porphyrin **3a** were measured in both absence and presence of fullerenes at the concentrations corresponding to those of the dimer (Figure S7 in SI). The negligible decreases of the fluorescence intensities exclude intermolecular quenching by fullerenes.[21] Therefore, the decreases of the fluorescence intensities of the free-base dimer by the addition of fullerenes are ascribed to the intramolecular quenching within the inclusion complexes. The association constants of the free-base dimers were obtained also from the fluorescence change by using eq 3, wherein F is ΔInt at 100% complexation. K_{assoc} and F were similarly treated as fitting parameters.

Upon addition of the fullerenes to the toluene solution of the cyclic dimers, their Soret bands were red-shifted, accompanied with reduced intensity (Figure 2 and Figures S2−S4 in SI). The Job plots upon mixing of the dimers and fullerenes confirm the formation of 1:1 host−guest complexes (Figure S8 in SI). On the basis of the titrations of the cyclic porphyrin dimers with C_{60} and C_{70} in toluene at 25 °C, the association constants (K_{assoc}) were determined by applying a nonlinear curve-fitting method using eq 1 or 2. Because C_{70} has non-negligible absorption near the Soret band region, eq 2 was used in the cases of C_{70}.

$$\Delta\mathrm{Abs} = \Delta\varepsilon \frac{[1 + K_{assoc}A + K_{assoc}X - \{(1 + K_{assoc}A + K_{assoc}X)^2 - 4K_{assoc}{}^2AX\}^{0.5}]}{2K_{assoc}} \quad (1)$$

$$\Delta\mathrm{Abs} = \varepsilon_{70}X + (\Delta\varepsilon - \varepsilon_{70}) \frac{1 + K_{assoc}A + K_{assoc}X - \{(1 + K_{assoc}A + K_{assoc}X)^2 - 4K_{assoc}{}^2AX\}^{0.5}}{2K_{assoc}} \quad (2)$$

$$\Delta\mathrm{Int} = F \frac{1 + K_{assoc}A + K_{assoc}X - \{(1 + K_{assoc}A + K_{assoc}X)^2 - 4K_{assoc}{}^2AX\}^{0.5}}{2K_{assoc}A} \quad (3)$$

dx.doi.org/10.1021/jo500034f | J. Org. Chem. 2014, 79, 2980−2992

Table 1. Association Constants (M^{-1}) of Cyclic Porphyrin Dimers for C_{60} and C_{70} in Toluene at 25 °C

	K_{assoc} for C_{60}		K_{assoc} for C_{70}	
host compound	absorption	fluorescence	absorption	fluorescence
H_4-Ptz-CPD$_{Py}$(OC_6)	$3.9 \pm 0.7 \times 10^6$	$4.5 \pm 0.7 \times 10^6$	[b] $> 10^7$	$7.4 \pm 0.8 \times 10^7$
Ni_2-Ptz-CPD$_{Py}$ (OC_6)	$1.3 \pm 0.2 \times 10^6$	[a]	[b] $> 10^7$	[a]
H_4-C_4-CPD$_{Py}$(OC_6)	$1.2 \pm 0.2 \times 10^5$	$9.8 \pm 1.0 \times 10^4$	$2.2 \pm 0.5 \times 10^5$	$1.4 \pm 0.2 \times 10^5$
Ni_2-C_4-CPD$_{Py}$(OC_6)	$2.9 \pm 0.4 \times 10^5$	[a]	$7.3 \pm 0.9 \times 10^5$	[a]

[a]Not determined due to no emission from nickel porphyrins. [b]Not determined due to high association constants over 10^7 M^{-1}.

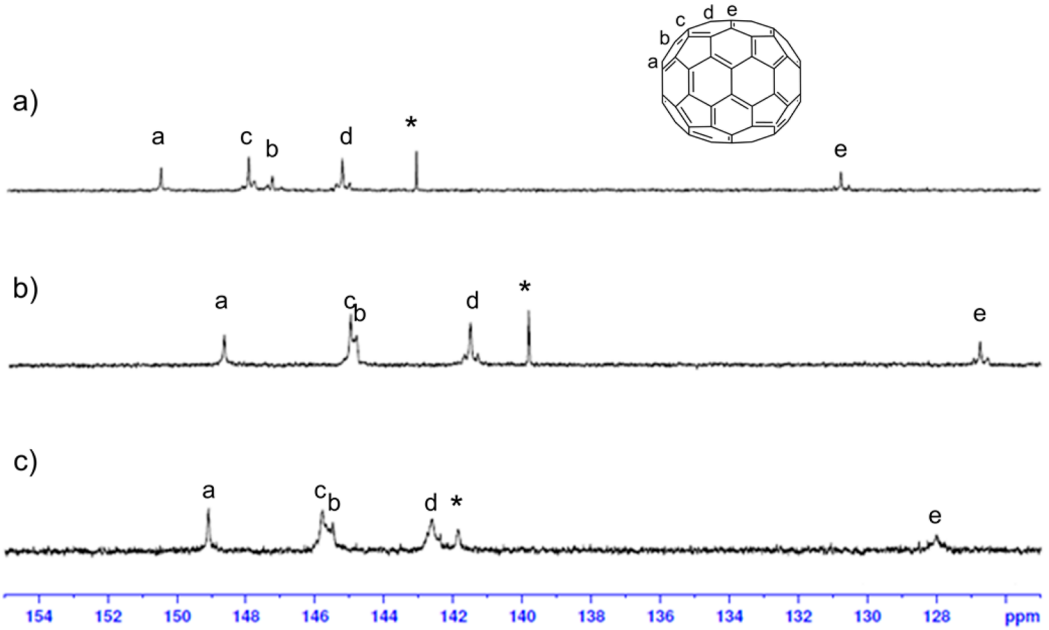

Figure 4. ^{13}C NMR spectra of (a) ^{13}C-enriched C_{70} (0.5 mM), (b) a mixture of H_4-Ptz-CPD$_{Py}$(OC_6) (0.5 mM) and ^{13}C-enriched C_{70} (0.5 mM), (c) a mixture of Ni_2-Ptz-CPD$_{Py}$(OC_6) (0.5 mM) and ^{13}C-enriched C_{70} (0.5 mM) in $CDCl_3/CS_2$ (1:1) at 25 °C. The asterisks indicate signals of contaminated C_{60}.

This fluorescence titration is valid even for K_{assoc} higher than 10^7 M^{-1}. The constants determined by fluorescence spectroscopy are acceptably close to those obtained by UV−vis absorption method. The association constants of phenothiazine-linked dimers are summarized in Table 1 along with those of the butadiyn-linked ones[12f] for comparison.

The K_{assoc} value of H_4-Ptz-CPD$_{Py}$(OC_6) for C_{60} ($3.9 \pm 0.7 \times 10^6$ M^{-1}) is much larger (over 30 times) than that of H_4-C_4-CPD$_{Py}$(OC_6) ($1.2 \pm 0.2 \times 10^4$ M^{-1}). In order to interpret this high affinity, the structure of H_4-Ptz-CPD$_{Py}$(H) was also optimized by DFT (M06-2X/6-31G(d,p) calculation.[16] H_4-Ptz-CPD$_{Py}$(H) has a slipped form of the two porphyrins (Figure S1 in SI), which conformation is similar to that of the crystal structure of H_4-C_4-CPD$_{Py}$(H).[12c] The dihedral angles between the *meso*-phenyl groups and the mean planes of the porphyrins are ca. 64° (Table S1 in SI). Upon C_{60} inclusion, these dihedral angles increase to ca. 88° to give a fully overlapped form of the two porphyrins, indicating that the inclusion occurs in an induced-fit fashion. However, there are only small changes in the center-to-center distance and the butterfly angles of the phenothiazine groups (Table S1 in SI). Hence, the high affinity of H_4-Ptz-CPD$_{Py}$(OC_6) to C_{60} would be derived mainly from the following two factors: i) the flexibility of the dihedral angles between the phenyl groups and the porphyrin planes, and ii) the suitable length of the phenothiazine bridges.

There have been free-base porphyrin hosts having relatively high C_{60} affinities such as the dimer by Aida et al. (7.9×10^5 M^{-1} in benzene)[4d] and the dimer by Zhang et al. (1.4×10^5 M^{-1} in toluene).[4t] To the best of our knowledge, H_4-Ptz-CPD$_{Py}$(OC_6) exhibited the highest C_{60} affinity among ever reported host molecules composed of free-base porphyrins. Even extending to metalloporphyrin-based hosts, there have been only four hosts having C_{60} affinity higher than 10^6 M^{-1}; the cobalt, rhodium and iridium dimers by Aida et al. (2.0×10^6, 2.5×10^7 and $>10^9$ M^{-1} in benzene, respectively)[4d,l] and the zinc trimer by Anderson et al. (1.6×10^6 M^{-1} in toluene).[4m] The extraordinary high C_{60} affinities of the rhodium and iridium dimers by Aida et al. are due to the assist of the specific carbophilicity of these metal ions, whose property is common for group IX metals. Based on these comparisons, the remarkably high C_{60} affinity of H_4-Ptz-CPD$_{Py}$(OC_6) implies that its phenothiazine-bridged structure is highly suitable for C_{60} inclusion.

The K_{assoc} value of Ni_2-Ptz-CPD$_{Py}$(OC_6) for C_{60} ($1.3 \pm 0.2 \times 10^6$ M^{-1}) is lower than that of the free-base counterpart ($3.9 \pm 0.7 \times 10^6$ M^{-1}). The less efficient inclusion of C_{60} would be derived from that its cavity size is slightly too large for C_{60} inclusion due to the distortion of the nickel porphyrins,[22] as suggested by the previous result that C_{60}⊂Ni_2-C_4-CPD$_{Py}$(H) has the longer center-to-center distance than the C_{60} complex of the corresponding free-base dimer.[12a,c]

Notably, the K_{assoc} value of H_4-Ptz-CPD$_{Py}$(OC_6) for C_{70} ($7.4 \pm 0.8 \times 10^7$ M^{-1}), which is significantly higher (ca. 500 times) than that of H_4-C_4-CPD$_{Py}$(OC_6) ($1.4 \pm 0.2 \times 10^5$ M^{-1}), reveals

dx.doi.org/10.1021/jo500034f | J. Org. Chem. 2014, 79, 2980−2992

that its molecular design is also effective for C_{70} inclusion. This result would be owing to the fact that the length of the shorter axis of C_{70} (7.1 Å) is almost the same as the diameter of C_{60}.[23] The K_{assoc} value of H_4-Ptz-$CPD_{Py}(OC_6)$ for C_{70} is one of the highest constants of porphyrin-based hosts, while there have been few better examples; the rhodium dimer by Aida et al. (1.0×10^8 M^{-1} in benzene),[4d] the zinc trimer by Anderson et al. (1.6×10^8 M^{-1} in toluene)[4m] and the free-base dimer by Zhang et al. (1.5×10^8 M^{-1} in toluene).[4t] Although the K_{assoc} value of Ni_2-Ptz-$CPD_{Py}(OC_6)$ for C_{70} could not be determined precisely, it is worth of noting that its C_{70} affinity is fairly high (over 10^7 M^{-1}) and appreciably improved by at least 15 times in comparison with that of Ni_2-C_4-$CPD_{Py}(OC_6)$ ($7.3 \pm 0.9 \times 10^5$ M^{-1}).

The electrospray inonization mass (ESI-MS) spectra of 1:1 mixtures of fullerenes and the cyclic porphyrin dimers in $CHCl_3$/MeOH/CH_3COOH (25/25/1) showed prominent ion peak clusters of the inclusion complexes (Figure S9 in SI), for example, at m/z = 1387.7 for $[H_4\text{-Ptz-CPD}_{Py}(OC_6) + C_{60}]^{2+}$ and m/z = 1444.5 for $[Ni_2\text{-Ptz-CPD}_{Py}(OC_6) + C_{60}]^{2+}$. These observations by ESI-MS spectroscopy also confirm the 1:1 inclusions of C_{60} and C_{70} within the present cyclic porphyrin dimers in solution, respectively.

The ^{13}C NMR spectra of 1:1 mixtures of ^{13}C-enriched fullerenes and the cyclic dimers in $CDCl_3/CS_2$ (1/1) exhibited high-field-shifted signals of the included fullerenes due to the ring current effects of the porphyrins (Figure 4 and Figure S10 in SI). Included C_{60} molecule shows one singlet signal due to its I_h symmetry and its very rapid rotation, while C_{70} gives five different signals (alphabetical labels are indicated in Figure 4). The chemical shifts (δ) and high-field shift values ($\Delta\delta$) in ppm are shown in Table 2 and 3. In general, high-field shifts of C_{70} signals are good indicators to clarify the C_{70} orientation with respect to a porphyrin plane.[4b,e,d,l,24] In the case of an end-on orientation, carbon atoms near the poles show larger high-field shifts (in absolute values). When C_{70} takes a side-on orientation, carbon atoms near the equator have larger high-field shifts. In the ^{13}C NMR spectra of all the present C_{70} inclusion complexes, carbon atoms near the equator exhibit larger high-field shifts than ones near the poles, implying that the side-on orientation of the C_{70} molecule is dominant in these inclusion complexes in solution.

Table 2. ^{13}C-NMR Data of Free and Included C_{60} in $CDCl_3/CS_2$ (1:1) at 25 °C

cmpd	δ	$\Delta\delta$
free C_{60}	143.1	
$C_{60}\subset H_4$-Ptz-$CPD_{Py}(OC_6)$	139.6	−3.5
$C_{60}\subset Ni_2$-Ptz-CPD_{Py} (OC_6)	141.3	−1.8

Table 3. ^{13}C-NMR Data of Free and Included C_{70} in $CDCl_3/CS_2$ (1:1) at 25 °C

cmpd	δ_a ($\Delta\delta$)	δ_b ($\Delta\delta$)	δ_c ($\Delta\delta$)	δ_d ($\Delta\delta$)	δ_e ($\Delta\delta$)
free C_{70}	150.5	147.2	148.0	145.3	130.8
$C_{70}\subset H_4$-Ptz-$CPD_{Py}(OC_6)$	148.8 (−1.7)	144.8 (−2.4)	145.1 (−2.9)	141.6 (−3.7)	126.8 (−4.0)
$C_{70}\subset Ni_2$-Ptz-CPD_{Py} (OC_6)	149.2 (−1.3)	145.5 (−1.7)	145.9 (−2.1)	142.7 (−2.6)	128.1 (−2.7)

Crystal Structure of the Inclusion Complex of C_{60} with H_4-Ptz-$CPD_{Py}(OC_3)$. We have successfully obtained single crystals of $C_{60}\subset H_4$-Ptz-$CPD_{Py}(OC_3)$ suitable for X-ray crystallographic analysis from $CHCl_3$/chlorobenzene solution by slow evaporation. The crystal structure clearly reveals 1:1 inclusion of C_{60} within the cavity of H_4-Ptz-$CPD_{Py}(OC_3)$ (Figure 5). This inclusion complex has a plane of symmetry between the two porphyrin moieties, which are equivalent to each other due to this plane. Therefore, the included C_{60} molecule can be regarded as the union of two equivalent hemispheres divided by this plane.

The two benzene rings of each phenothiazine moiety are equivalent to each other and the nitrogen, sulfur, and methyl carbon atoms are on the symmetry plane. Two pairs of the pyridyl groups are treated as disordered structures. Additionally, two pairs of the propyl groups outside the cavity were modeled as two disordered structures.

Though the porphyrin planes are almost planar, the *meso*-carbons are slightly displaced from the mean plane of the four pyrrole nitrogens. The pyridyl-substituted *meso*-carbons show larger inward displacements (0.107 and 0.214 Å) than the phenyl-substituted ones shifting outward (0.007 and 0.026 Å). The two phenothiazine groups have butterfly structures; the dihedral angles between the two phenyl rings are 150.83° and 151.26°. The C_{60} molecule is located just above the centers of the porphyrins, exhibiting a large difference from the off-center location of C_{60} in the crystal structure of $C_{60}\subset Ni_2$-C_4-$CPD_{Py}(H)$ which has a shorter separation between the two opposite phenyl rings connected to linker groups.[25] The 6:6 ring-juncture C−C bond at each pole of C_{60} is closest to the porphyrin as in most examples of C_{60}-porphyrin cocrystals.[3a] This C−C bond has near alignment with a *trans* N···N vector with a short separation (2.830 Å) between the closest C_{60} carbon and the porphyrin center (Figure 6), suggesting a strong $\pi-\pi$ interaction of the two π-systems. The two porphyrins are almost parallel to each other, and the center-to-center distance is 12.454 Å. This value is in the quite favorable range for C_{60} inclusion as predicted in the molecular design. Hence, it is rational to assign the remarkably high C_{60} affinity of H_4-Ptz-$CPD_{Py}(OC_6)$ in solution to these structural features of $C_{60}\subset H_4$-Ptz-$CPD_{Py}(OC_3)$.

Most interestingly, a desired self-assembled porphyrin nanotube is observed in the crystal packing of $C_{60}\subset H_4$-Ptz-$CPD_{Py}(OC_3)$ as seen in the case of $C_{60}\subset Ni_2$-C_4-CPD_{Py}[12a] (Figure 7). The tubular structure is formed by multiple cooperative noncovalent interactions between each dimer; a pair of complementary C−H···N hydrogen-bonding interactions between the pyrrole β-CH and nitrogen atoms of the pyridyl groups with C···N distances of 3.38(1) and 3.40(1) Å for the major ones of the disordered pyridyl groups (Figure 8; for the minor pyridyl groups, see Figure S11 in SI). The second interaction is a weak $\pi-\pi$ interaction between the *meso*-pyridyl groups; the shortest C−C distances of 3.75(1) Å and the dihedral angle of 5.00° are confirmed. The C_{60} molecules are linearly arranged inside the channel of the nanotube with the distance between the C_{60} centers of 14.794 Å, which is slightly longer than that of $C_{60}\subset Ni_2$-C_4-$CPD_{Py}(H)$ (14.498 Å). It is noteworthy that this self-assembly for the porphyrin nanotube including the C_{60} linear array is induced by the *meso*-pyridyl groups irrespective of central metal ions (nickel and free-base) and linkage groups (butadiynyl and phenothiazine).

■ CONCLUSION

In order to construct efficient and nanotube-forming hosts for fullerenes, we have designed and prepared free-bases and a

dx.doi.org/10.1021/jo500034f | J. Org. Chem. 2014, 79, 2980−2992

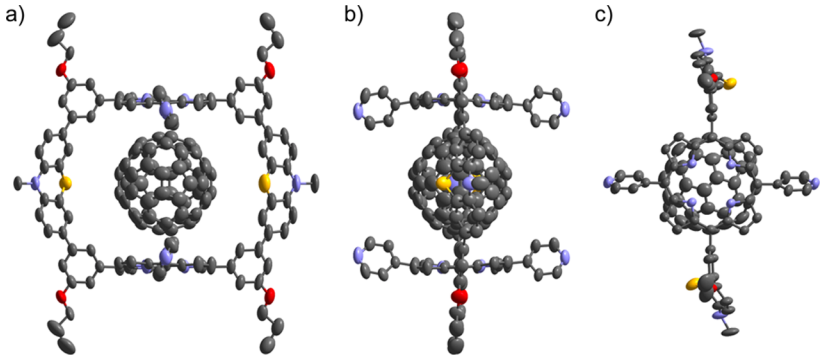

Figure 5. ORTEP drawing of C_{60}⊂H_4-Ptz-$CPD_{Py}(OC_6)$ with 50% probability thermal ellipsoids. Hydrogen atoms, disordered structures, and solvent molecules are omitted for clarity. (a) Front view; (b) side view; (c) top view.

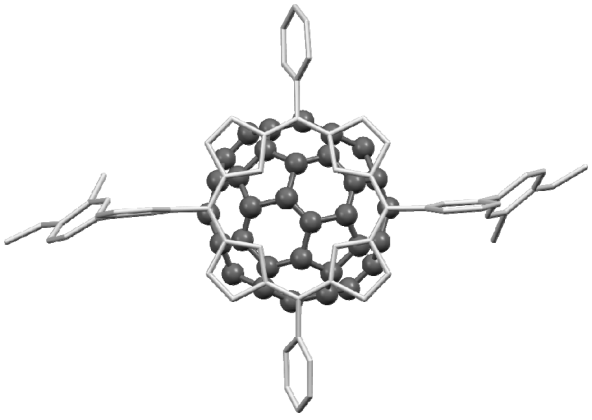

Figure 6. Orientation of the 6:6 ring-juncture of C_{60} over the porphyrin center.

nickel complex of cyclic porphyrin dimers having self-assembling 4-pyridyl groups and phenothiazine linkers at the opposite *meso*-positions. The porphyrin dimers have been obtained by Suzuki−Miyaura cross-coupling of dihalogenated porphyrins and bisborylated phenothiazine derivative. The phenothiazine-bridged free-base dimer, H_4-Ptz-$CPD_{Py}(OC_6)$, showed very high affinities for fullerenes such as $K_{assoc} = 3.9 \pm 0.7 \times 10^6$ M^{-1} for C_{60} and $K_{assoc} = 7.4 \pm 0.8 \times 10^7$ M^{-1} for C_{70}. This C_{60} affinity is the highest value ever reported among host molecules composed of free-base porphyrins, indicating that H_4-Ptz-$CPD_{Py}(OC_6)$ has an optimum molecular cavity for C_{60} inclusion. On the other hand, the C_{60} affinity of Ni_2-Ptz-$CPD_{Py}(OC_6)$ ($1.3 \pm 0.2 \times 10^6$ M^{-1}) is lower than that of H_4-Ptz-$CPD_{Py}(OC_6)$ probably due to the slightly larger size of its cavity. The association constant of Ni_2-Ptz-$CPD_{Py}(OC_6)$ for C_{70} is, however, found to be over 10^7 M^{-1}. The ^{13}C NMR spectra of the C_{70} inclusion complexes suggest that the included C_{70} molecule adopts mainly a side-on orientation within the cavity of these cyclic dimers. X-ray crystallographic analysis of C_{60}⊂H_4-Ptz-$CPD_{py}(OC_3)$ revealed that the included C_{60} molecule is localized just above the centers of the porphyrin moieties due to the strong $\pi-\pi$ interaction. The two porphyrin planes are almost parallel to each other, and the center-to-center distance (12.454 Å) was found to be quite suitable for C_{60} inclusion. The very high C_{60} affinity of H_4-Ptz-$CPD_{py}(OC_6)$ is rationally assigned to these structural features revealed by X-ray crystallography. Along with our expectation, C_{60}⊂H_4-Ptz-$CPD_{py}(OC_3)$ forms a self-assembled nanotube through porphyrin β-C−H···N_{Py} hydrogen bonds and $\pi-\pi$ stackings of the *meso*-pyridyl groups in the crystal packing of this inclusion complex. The C_{60} molecules are linearly aligned in the inner channel of this nanotube to produce a supramolecular peapod. Further electrochemical and photophysical studies of these supramolecular architectures are now in progress.

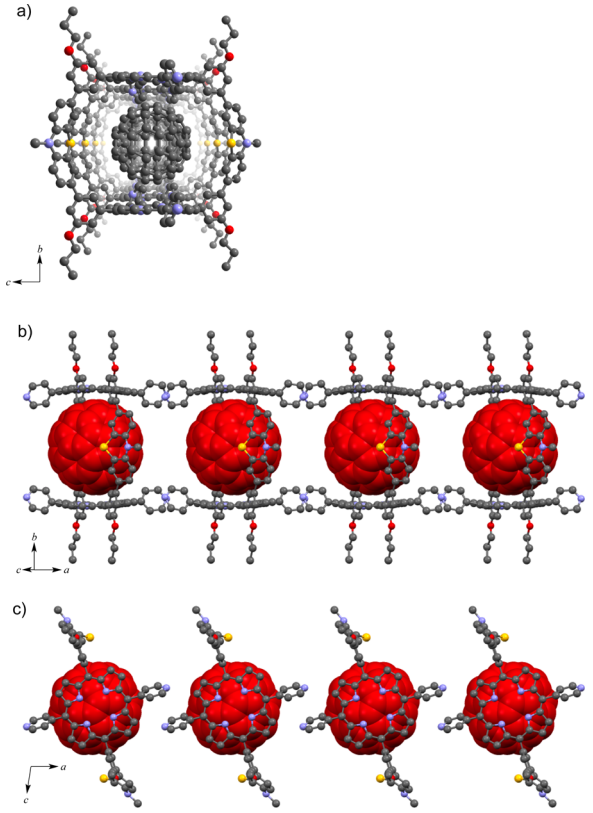

Figure 7. Tubular assembly and linear array of C_{60} in the crystal packing of C_{60}⊂H_4-Ptz-$CPD_{Py}(OC_3)$. (a) Front view; (b) side view; (c) top view.

EXPERIMENTAL SECTION

General Information. Reagents and solvents of best grade available were purchased from commercial suppliers and were used without further purification unless otherwise noted. *N*,*N*-Dimethylformamide (DMF) was purified by distillation from CaH_2 under reduced pressure. Dry tetrahydrofuran (THF) was obtained by distillation from Na and benzophenone under N_2 atmosphere. Analytical thin-layer chromatography (TLC) was

dx.doi.org/10.1021/jo500034f | J. Org. Chem. 2014, 79, 2980−2992

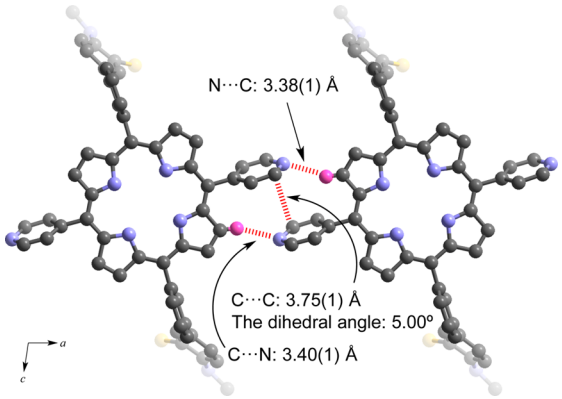

Figure 8. Details of the noncovalent interactions linking the cyclic porphyrin dimers in the crystal of C_{60}⊂H_4-Ptz-$CPD_{py}(OC_3)$. The major parts of the disordered pyridyl groups are shown. Hydrogen atoms are omitted except in the C−H···N moieties. N = purple; C = gray; H = pink; S = yellow.

performed on silica gel 60 F_{254} precoated aluminum sheets. Colunm chromatography was carried out using silica gel (63-210 mesh) or florisil (60−120 mesh). Chemical shifts of nuclear magnetic resonance (NMR) spectra were reported as δ values in ppm relative to tetramethylsilane. High-resolution fast atom bombardment mass spectra (HR-FAB-MS) were measured with 3-nitrobenzyl alcohol (NBA) or a mixture of dithiothreitol and dithioerythritol (Magic Bullet) as a matrix and recorded on a double-focusing magnetic sector mass spectrometer. Recycling preparative GPC-HPLC was carried out with $CHCl_3$/NEt_3 (100:1) as an eluent at a flow rate of 3.5 mL/min. The computation was carried out using the computer facilities at Research Institute for Information Technology, Kyushu University.

X-ray Structure Determination. The free-base dimer (H_4-Ptz-$CPD_{Py}(OC_3)$) in $CHCl_3$ (0.01 mM, 1 mL) and C_{60} in chlorobenzene (0.01 mM, 1 mL) were mixed in a loosely closed vial and stored in the dark at room temperature. The slow and preferential evaporation of chloroform afforded single crystals due to the lower solubility of the inclusion complex in chlorobenzene. X-ray crystallography was carried out on a single crystal of C_{60}⊂H_4-Ptz-$CPD_{Py}(OC_3)$ with a monochromated synchrotoron radiation (λ = 0.7104 Å) at SPring-8 BL02B1. Reflection data were corrected for Lorentz and polarization effects. The structure was solved by a direct method (SIR-2004)[26] with the Crystal Structure[27] crystallographic software package, and refined by full-matrix least-squares procedures on F^2 for all reflections (SHELXL-97).[28] Non-hydrogen atoms were refined anisotropically. Hydrogen atoms were refined by using the rigid model. Some solvent molecules, such as chloroform and chlorobenzene were not properly modeled due to their disorder. Therefore, the structure was refined without these solvents by PLATON Squeeze technique.[29] The final structure was validated by using PLATON cif check. Crystallographic data for C_{60}⊂H_4-Ptz-$CPD_{Py}(OC_3)$: $C_{122}H_{94}N_{14}O_4S_2{\cdot}C_{60}$, brown prismatic crystal, crystal dimensions 0.08 × 0.05 × 0.06 mm^3, monoclinic, $P2_1/m$, a = 14.794(19) Å, b = 32.47(5) Å, c = 17.79(3) Å, β = 100.281(16)°, V = 8410(22) $Å^3$, Z = 2, ρ_{calc} = 1.029 g cm^{-3}, $2\theta_{max}$ = 54.10°, T = 123 K, 79175 reflections collected; 19368 reflections used and 1091 parameters. R_1 = 0.0832 [$I > 2.0\sigma(I)$], R_w = 0.2384 (all data). Crystallographic data have been deposited with Cambridge Crystallographic Date Centre: Deposition number CCDC-973900. Copies of the date can be obtained free of charge via http://www.ccdc.cam.ac.uk/conts/retrieving.html (or from the Cambridge Crystallographic Date Centre, 12, Union Road, Cambridge, CB2 1EZ, U.K.; fax: +44 1223 336033; e-mail: deposit@ccdc.cam.ac.uk)

*1,3-Dibromo-5-(propyloxy)benzene (**1b**).* A mixture of 3,5-dibromophenol[30] (17.0 g, 67.5 mmol), 1-bromopropane (9.83 g, 80.0 mmol) and K_2CO_3 (13.8 g, 100 mmol) in 2-butanone (150 mL) was heated to reflux under N_2 atmosphere overnight. After cooling, water (300 mL) and $CHCl_3$ (300 mL) were added. The organic phase was separated, and the aqueous phase was extracted with $CHCl_3$ (100 mL × 2). The combined organic phase was dried with Na_2SO_4 and evaporated in *vacuo*. The crude product was purified by column chromatography (silica gel, hexane) to give colorless oil (18.4 g, 89%). ^{1}H NMR (400 MHz, $CDCl_3$): δ 7.23 (s, 1H, Ar−H), 6.99 (s, 2H, Ar−H), 3.88 (t, J = 6.6 Hz, 2H, OCH_2), 1.79 (sext, J = 7.2 Hz, 2H, $OCH_2\underline{CH_2}CH_3$), 1.02 (t, J = 7.2 Hz, 3H, CH_3); ^{13}C NMR ($CDCl_3$, 150 MHz): δ 160.5 (aromatic C), 126.3 (aromatic C), 123.2 (aromatic C), 117.1 (aromatic C), 70.3 (OCH_2), 22.5 (CH_2), 10.6 (CH_3); IR (oil): ν = 3080, 2966, 2937, 2877, 1583, 1568, 1439, 1419, 1339, 1298, 1255, 1230, 1107, 1088, 1066, 1046, 1022, 987, 889, 853, 829, 744, 669 cm^{-1}; HR-FAB-MS (NBA): m/z calcd for $C_9H_{11}Br_2O$: 292.9177; found: 292.9149.

*3-Bromo-5-(propyloxy)benzaldehyde (**2b**).* 1,3-Dibromo-5-(propyloxy)benzene **1b** (2.94 g, 10.0 mmol) was added into a three-neck flask, and the flask was filled with N_2. Then, dry THF (100 mL) was added into the flask under N_2 atmosphere, and the solution was cooled to −78 °C. Then, *n*-butyllithium (2.69 M solution in *n*-hexane, 3.7 mL, 10 mmol) was added dropwise to the solution. After 1 h, excess DMF was added to the mixture. After warming to room temperature, the reaction mixture was quenched with water. The separated organic phase was washed with water (100 mL, 2 times), and dried over Na_2SO_4 and evaporated *in vacuo*. The crude product was purified by column chromatography (silica gel, *n*-hexane/$CHCl_3$, 3:1) to furnish the product as a light-yellow oil (1.87 g, 77%). ^{1}H NMR (600 MHz, $CDCl_3$): δ 9.89 (s, 1H, CHO), 7.55 (t, J = 1.6 Hz, 1H, Ar−H), 7.30 (m, 2H, Ar−H), 3.96 (t, J = 6.6 Hz, 2H, OCH_2), 1.81 (sext, J = 7.2 Hz, 2H, $OCH_2\underline{CH_2}CH_3$), 1.04 (t, J = 7.2 Hz, 3H, CH_3); ^{13}C NMR ($CDCl_3$, 150 MHz): δ 190.8 (CHO), 160.7 (aromatic C), 139.1 (aromatic C), 125.6 (aromatic C), 124.5 (aromatic C), 123.8 (aromatic C), 113.2 (aromatic C), 70.6 (OCH_2), 22.8 (CH_2), 10.8 (CH_3); IR (oil): ν = 3385, 3078, 2966, 2937, 2879, 2725, 2409, 2289, 1705, 1591, 1590, 1452, 1383, 1317, 1273, 1246, 1151, 1099, 1065, 953, 939, 849, 690, 671 cm^{-1}; HR-FAB-MS (NBA): m/z calcd for $C_{10}H_{12}BrO_2$: 243.0021; found: 243.0021.

*5,15-Bis[3-bromo-5-(hexyloxy)phenyl]-10,20-di[4-pyridyl]-porphine (**3a**).* A solution of 3-Bromo-5-(hexyloxy)-benzaldehyde[12f] **2a** (570 mg, 2.00 mmol) and *meso*-(4-pyridyl)dipyrromethane[18] (446 mg, 2.00 mmol) in 200 mL CH_2Cl_2 was purged with N_2 for 15 min and shielded from light. To the solution, trifluoroacetic acid (1.86 mL, 25.0 mmol) was added, and the solution was stirred for 30 min at room temperature. Then 2,3-dichloro-5,6-dicyano-1,4-benzoquinone (680 mg, 3.00 mmol) dissolved in THF was added to the solution; the resulting solution was stirred for an additional 1 h. The reaction mixture was neutralized with triethylamine (3.36 mL, 24.1 mmol). After evaporation, the mixture was purified by column chromatography (silica gel, $CHCl_3$/EtOH, 100:1 to $CHCl_3$/EtOH, 50:1). The crude product was washed with

dx.doi.org/10.1021/jo500034f | J. Org. Chem. 2014, 79, 2980−2992

MeOH and dried *in vacuo* to give the porphyrin as a purple powder (98 mg, 10%). Mp: >300 °C; ^{1}H NMR (600 MHz, $CDCl_3$): δ 9.05 (d, J = 4.8 Hz, 4H, Ar−H), 8.95 (d, J = 4.2 Hz, 4H, pyrrole β-H), 8.82 (d, J = 4.2 Hz, 4H, pyrrole β-H), 8.16 (d, J = 5.4 Hz, 4H, Ar−H), 7.94 (s, 2H, Ar−H), 7.69 (s, 2H, Ar−H), 7.51 (s, 2H, Ar−H), 4.14 (t, J = 6.6 Hz, 4H, OCH_2), 1.87 (quin, J = 6.6 Hz, 4H, $OCH_2\underline{CH_2}(CH_2)_3CH_3$), 1.53−1.46 (m, 4H, $O(CH_2)_2\underline{CH_2}(CH_2)_2CH_3$), 1.38−1.32 (m, 8H, $O(CH_2)_3\underline{(CH_2)_2}CH_3$), 0.90 (t, J = 6.6 Hz, 6H, CH_3), −2.92 (br s, 2H, NH); ^{13}C NMR (150 MHz, $CDCl_3$): δ 158.3 (aromatic C), 150.2 (aromatic C), 148.5 (aromatic C), 144.4 (aromatic C), 130.1 (aromatic C), 129.5 (aromatic C), 121.4 (aromatic C), 120.6 (aromatic C), 120.6 (aromatic C), 119.3 (aromatic C), 117.7 (aromatic C), 117.5 (aromatic C), 68.9 (OCH_2), 31.7 (CH_2), 29.3 (CH_2), 25.9 (CH_2) 22.7 (CH_2), 14.2 (CH_3); IR (KBr): ν = 3317, 2929, 2869, 1591, 1474, 1426, 1350, 1269, 1171, 1050, 975, 921, 859, 800, 730, 659 cm^{-1}; UV−vis ($CHCl_3$): λ_{max} (ε, cm^{-1} M^{-1}) = 419 (467500), 514 (21250), 547 (6150), 588 (6300), 646 (3400) nm; HR-FAB-MS (NBA): m/z calcd for $C_{54}H_{50}Br_2N_6O_2$: 972.2362; found 972.2369.

*5,15-Bis[3-bromo-5-(propyloxy)phenyl]-10,20-di[4-pyridyl]porphine (**3b**).* A solution of 3-bromo-5-(propyloxy)-benzaldehyde **2b** (486 mg, 2.00 mmol) and *meso*-(4-pyridyl)-dipyrromethane[18] (446 mg, 2.00 mmol) in 200 mL of CH_2Cl_2 was purged with N_2 for 15 min and shielded from light. To the solution was added trifluoroacetic acid (1.86 mL, 25.0 mmol), and the solution was stirred for 30 min at room temperature. Then 2,3-dichloro-5,6-dicyano-1,4-benzoquinone (680 mg, 3.00 mmol) dissolved in THF was added to the solution; the resulting solution was stirred for an additional 1 h. The reaction mixture was neutralized with triethylamine (3.36 mL, 24.1 mmol). After evaporation, the mixture was purified by column chromatography (silica gel, $CHCl_3$/EtOH, 100:1 to $CHCl_3$/EtOH, 50:1). The crude product was washed with MeOH and dried *in vacuo* to give the porphyrin as a purple powder (80 mg, 9%). Mp: >300 °C; ^{1}H NMR (600 MHz, $CDCl_3$): δ 9.05 (d, J = 4.8 Hz, 4H, Ar−H), 8.95 (d, J = 4.2 Hz, 4H, pyrrole β-H), 8.82 (d, J = 4.2 Hz, 4H, pyrrole β-H), 8.16 (d, J = 5.4 Hz, 4H, Ar−H), 7.94 (s, 2H, Ar−H), 7.70 (s, 2H, Ar−H), 7.51 (s, 2H, Ar−H), 4.12 (t, J = 6.6 Hz, 4H, OCH_2), 1.90 (sext, J = 7.2 Hz, 4H, $OCH_2\underline{CH_2}CH_3$), 1.09 (t, J = 7.2 Hz, 6H, CH_3), −2.92 (br s, 2H, NH); ^{13}C NMR (150 MHz, $CDCl_3$): δ 158.7 (aromatic C), 150.6 (aromatic C), 149.0 (aromatic C), 144.8 (aromatic C), 130.6 (aromatic C), 130.0 (aromatic C), 121.9 (aromatic C), 121.0 (aromatic C), 119.7 (aromatic C), 118.1 (aromatic C), 118.0 (aromatic C), 70.8 (OCH_2), 23.2 (CH_2), 11.1 (CH_3); IR (KBr): ν = 3317, 2934, 2876, 1592, 1475, 1426, 1350, 1269, 1172, 1051, 973, 927, 859, 800, 730, 659 cm^{-1}; UV−vis ($CHCl_3$): λ_{max} (ε, cm^{-1} M^{-1}) = 419 (444000), 514 (21250), 547 (6450), 589 (6380), 647 (3150) nm; HR-FAB-MS (NBA): m/z calcd for $C_{48}H_{39}N_6Br_2O_2$: 889.1501; found: 889.1504.

*{5,15-Bis[3-bromo-5-(hexyloxy)phenyl]-10,20-di[4-pyridyl]porphinato}Ni(II) (**4a**).* A solution of $Ni(OAc)_2{\cdot}4H_2O$ (496 mg, 2.00 mmol) in MeOH (20 mL) was added to a solution of **3a** (195 mg, 0.200 mmol) in $CHCl_3$ (100 mL) and refluxed under N_2 for 1 day. The reaction mixture was diluted with $CHCl_3$ and washed with water (200 mL) twice. The organic layer was dried over Na_2SO_4, and the solvent was evaporated. The crude product was recrystallized from $CHCl_3$/MeOH to give **4a** as an orange powder (142 mg, 69%). Mp: >300 °C; ^{1}H NMR (400 MHz, $CDCl_3$): δ 8.97 (br s, 4H, Ar−H), 8.84 (d, J = 4.8 Hz, 4H, pyrrole β-H), 8.71 (d, J = 4.8 Hz, 4H, pyrrole β-H), 7.96 (d, J = 4.8 Hz, 4H, Ar−H), 7.75 (s, 2H, Ar−H), 7.48 (s, 2H, Ar−H), 7.43 (s, 2H, Ar−H), 4.08 (t, J = 6.6 Hz, 4H, OCH_2), 1.84 (quin, J = 7.2 Hz, 4H, $OCH_2\underline{CH_2}(CH_2)_3CH_3$), 1.51−1.44 (m, 4H, $O(CH_2)_2\underline{CH_2}(CH_2)_2CH_3$), 1.38−1.30 (m, 8H, $O(CH_2)_3\underline{(CH_2)_2}CH_3$), 0.89 (t, J = 6.6 Hz, 6H, CH_3); ^{13}C NMR (150 MHz, $CDCl_3$): δ 158.4 (aromatic C), 149.0 (aromatic C), 148.7 (aromatic C), 143.2 (aromatic C), 142.9 (aromatic C), 142.1 (aromatic C), 133.0 (aromatic C), 132.1 (aromatic C), 129.2 (aromatic C), 128.7 (aromatic C), 121.6 (aromatic C), 119.7 (aromatic C), 118.2 (aromatic C), 117.7 (aromatic C), 116.5 (aromatic C), 68.8 (OCH_2), 31.7 (CH_2), 29.3 (CH_2), 25.8 (CH_2) 22.7 (CH_2), 14.2 (CH_3); IR (KBr): ν = 2928, 2858, 1593, 1427, 1352, 1273, 1182, 1077, 1007, 867, 769, 713, 672 cm^{-1}; UV−vis ($CHCl_3$): λ_{max} (ε, cm^{-1} M^{-1}) = 415 (268250), 527 (18400) nm; HR-FAB-MS (NBA): m/z calcd for $C_{54}H_{48}Br_2N_6NiO_2$: 1028.1559; found: 1028.1533.

*10-Methyl-3,7-bis(4,4,5,5-tetramethyl-1,3,2-dioxaborolan-2-yl)-10H-phenothiazine (**5**).* 10-Methyl-3,7-dibromo-10*H*-phenothiazine[20] (834 mg, 2.25 mmol) was added into a three-neck flask, and the air inside of the flask was replaced with N_2. Then, dry THF (10 mL) was added into the flask, and the solution was cooled to −78 °C. Then, *n*-butyllithium (2.69 M solution in *n*-hexane, 2.1 mL, 5.6 mmol) was added dropwise to the solution. After stirring for 1 h, 2-isopropoxy-4,4,5,5-tetramethyl-1,3,2-dioxaborolane (1.82 mL, 8.92 mmol) was added to the reaction mixture. After warming to room temperature, the reaction mixture was quenched with water. The reaction mixture was extracted with CH_2Cl_2, dried over Na_2SO_4, and evaporated. The crude product was purified by column chromatography (silica gel, *n*-hexane/CH_2Cl_2, 1:1 then CH_2Cl_2) to furnish the product as a colorless powder (633 mg, 60%). Mp: 259−260 °C; ^{1}H NMR (500 MHz, $CDCl_3$): δ 7.57 (d, J = 8.6 Hz, 2H, Ar−H), 7.53 (s, 2H, Ar−H), 6.77 (d, J = 8.6 Hz, 2H, Ar−H), 3.38 (s, 3H, NCH_3), 1.32 (s, 24H, CH_3); ^{13}C NMR (150 MHz, $CDCl_3$): δ 147.9 (aromatic C), 134.5 (aromatic C), 133.6 (aromatic C), 122.8 (aromatic C), 113.7 (aromatic C), 83.8 (B−O−C), 35.6 (NCH_3), 25.0 (CH_3); IR (KBr): ν = 2983, 2933, 1605, 1583, 1408, 1389, 1375, 1354, 1298, 1261, 1211, 1169, 1146, 1130, 1115, 1105, 966, 858, 739, 692, 669 cm^{-1}; UV−vis (THF): λ_{max} (ε, cm^{-1} M^{-1}) = 270 (57000), 326 (5200) nm; HR-FAB-MS (NBA): m/z calcd for $C_{25}H_{33}O_4NB_2S$: 465.2316; found: 465.2308; Elemental analysis (%) calcd for $C_{25}H_{33}B_2NO_4S$: C 64.54 H 7.15 N 3.01; found: C 64.57 H 7.14 N 2.99.

H_4-Ptz-CPD$_{Py}$(OC$_6$). A THF/H_2O (40 mL, THF/H_2O, 10/1) solution of **3a** (97 mg, 0.10 mmol), **5** (47 mg, 0.10 mmol), $Pd(PPh_3)_4$ (46 mg, 0.040 mmol), and Cs_2CO_3 (325 mg, 1.00 mmol) was purged with N_2 for 30 min. The mixture was refluxed for 2 days under N_2 in the dark. After cooling to room temperature and evaporation, the reaction mixture was diluted with $CHCl_3$/NEt_3 ($CHCl_3$/NEt_3, 100:1) and washed with water (50 mL) twice. The organic layer was dried over Na_2SO_4 and evaporated. The residue was passed through short column chromatography (florisil, $CHCl_3$/NEt_3, 100:1). After evaporation of the solvent, the crude product was passed through gel permeation chromatography ($CHCl_3$/NEt_3, 100/1 as an eluent) and recrystallized from $CHCl_3$/MeOH to give the dimer as a purple powder (4.8 mg, 5%). Mp: >300 °C; ^{1}H NMR (600 MHz, $CDCl_3$): δ 8.96 (br s, 4H, Ar−H), 8.90 (br s, 4H, Ar−H), 8.87 (d, J = 4.2 Hz, 8H, pyrrole β-H), 8.66 (d, J = 4.2 Hz, 8H, pyrrole β-H), 8.04 (br s, 4H, Ar−H), 7.94 (br-s,

dx.doi.org/10.1021/jo500034f | J. Org. Chem. 2014, 79, 2980−2992

4H, Ar−H), 7.80 (s, 4H, Ar−H), 7.69 (d, J = 8.4 Hz, 4H, Ar−H), 7.65 (s, 4H, Ar−H), 7.46 (s, 4H, Ar−H), 7.29 (s, 4H, Ar−H), 6.98 (d, J = 8.4 Hz, 4H, Ar−H), 4.14 (t, J = 8.0 Hz, 8H, OCH_2), 3.52 (s, 6H, NCH_3), 1.86 (quin, J = 7.2 Hz, 8H, $OCH_2\underline{CH_2}(CH_2)_3CH_3$), 1.51 (m, 8H, $O(CH_2)_2\underline{CH_2}(CH_2)_2CH_3$), 1.31 (m, 16H, $O(CH_2)_3\underline{(CH_2)_2}CH_3$), 0.90 (t, J = 6.6 Hz, 12H, CH_3), −3.08 (br s, 4H, NH); IR (KBr): ν = 3317, 2927, 2868, 1590, 1480, 1430, 1262, 1055, 975, 921, 800, 725, 661 cm^{-1}; UV−vis ($CHCl_3$): λ_{max} (ε, cm^{-1} M^{-1}) = 418 (601900), 515 (32566), 549 (10100), 590 (9300), 647 (6200) nm; HR-FAB-MS (NBA): m/z calcd for $C_{134}H_{118}N_{14}O_4S_2$: 2050.8902; found 2050.8921; ^{13}C NMR spectrum could not be obtained due to the low solubility.

H_4-Ptz-CPD$_{Py}$(OC$_3$). A THF/H_2O (40 mL, THF/H_2O, 10/1) solution of **3b** (89 mg, 0.10 mmol), **5** (47 mg, 0.10 mmol), $Pd(PPh_3)_4$ (46 mg, 0.040 mmol), and Cs_2CO_3 (325 mg, 1.00 mmol) was purged with N_2 for 30 min. The mixture was refluxed for 2 days under N_2 in the dark. After cooling to room temperature and evaporation, the reaction mixture was diluted with $CHCl_3$/NEt_3 ($CHCl_3$/NEt_3, 100:1) and washed with water (50 mL) twice. The organic layer was dried over Na_2SO_4 and evaporated. The residue was passed through short column chromatography (florisil, $CHCl_3$/NEt_3, 100:1). After evaporation of the solvent, the crude product was passed through gel permeation chromatography ($CHCl_3$/NEt_3, 100/1 as an eluent) and recrystallized from $CHCl_3$/MeOH to give the dimer as a purple powder (2 mg, 2%). Mp: >300 °C; ^1H NMR (600 MHz, $CDCl_3$): δ 8.95 (br s, 4H, Ar−H), 8.90 (br s, 4H, Ar−H), 8.87 (d, J = 4.2 Hz, 8H, pyrrole β-H), 8.66 (d, J = 4.2 Hz, 8H, pyrrole β-H), 8.04 (br s, 4H, Ar−H), 7.93 (br s, 4H, Ar−H), 7.80 (s, 4H, Ar−H), 7.69 (d, J = 7.2 Hz, 4H, Ar−H), 7.65 (s, 4H, Ar−H), 7.46 (s, 4H, Ar−H), 7.29 (s, 4H, Ar−H), 6.98 (d, J = 8.4 Hz, 4H, Ar−H), 4.11 (t, J = 6.6 Hz, 8H, OCH_2), 3.52 (s, 6H, NCH_3), 1.89 (sext, J = 7.2 Hz, 8H, $OCH_2\underline{CH_2}CH_3$), 1.07 (t, J = 7.2 Hz, 12H, CH_3), −3.08 (br s, 4H, NH); IR (KBr): ν = 3317, 2963, 2876, 1589, 1480, 1430, 1262, 1068, 974, 930, 800, 731, 689 cm^{-1}; UV−vis ($CHCl_3$): λ_{max} (ε, cm^{-1} M^{-1}) = 418 (666700), 515 (38200), 549 (13000), 588 (11700), 647 (7100) nm.; HR-FAB-MS (Magic Bullet): m/z calcd for $C_{122}H_{95}N_{14}O_4S_2$: 1883.7102; found: 1883.7078; ^{13}C NMR spectrum could not be obtained due to the low solubility.

Ni$_2$-Ptz-CPD$_{Py}$(OC$_6$). A THF/H_2O (40 mL, THF/H_2O, 10/1) solution of **4a** (103 mg, 0.100 mmol), **5** (47 mg, 0.10 mmol), $Pd(PPh_3)_4$ (46 mg, 0.040 mmol), and Cs_2CO_3 (325 mg, 1.00 mmol) was purged with N_2 for 30 min. The mixture was refluxed for 2 days under N_2 in the dark. After cooling to room temperature and evaporation, the reaction mixture was diluted with $CHCl_3$/NEt_3 ($CHCl_3$/NEt_3, 100:1) and washed with water (50 mL) twice. The organic layer was dried over Na_2SO_4 and evaporated. The residue was passed through short column chromatography (florisil, $CHCl_3$/NEt_3, 100:1). After evaporation of the solvent, the crude product passed through gel permeation chromatography ($CHCl_3$/NEt_3, 100/1 as an eluent) and was recrystallized from $CHCl_3$/MeOH to give the dimer as a purple powder (5 mg, 5%). Mp: >300 °C; ^1H NMR (600 MHz, $CDCl_3$): ^1H NMR (600 MHz, $CDCl_3$): δ 8.89 (br s, 8H, Ar−H), 8.81 (d, J = 4.2 Hz, 8H, pyrrole β-H), 8.59 (d, J = 4.2 Hz, 8H, pyrrole β-H), 7.87 (br s, 8H, Ar−H), 7.74 (s, 4H, Ar−H), 7.63 (d, J = 8.4 Hz, 4H, Ar−H), 7.43 (m, 8H, Ar−H), 7.16 (s, 4H, Ar−H), 6.91 (d, J = 8.4 Hz, 4H, Ar−H), 4.17 (t, J = 6.6 Hz, 8H, OCH_2), 3.46 (s, 6H, NCH_3), 1.89 (quin, J = 7.2 Hz, 8H, $OCH_2\underline{CH_2}(CH_2)_3CH_3$), 1.51 (m, 8H, $O(CH_2)_2\underline{CH_2}(CH_2)_2CH_3$), 1.35 (m, 16H, $O(CH_2)_3\underline{(CH_2)_2}CH_3$), 0.89 (t, J = 6.6 Hz, 12H, CH_3); IR (KBr): ν = 2928, 2868, 1592, 1480, 1430, 1355, 1262, 1180, 1077, 1006, 867, 799, 713 cm^{-1}; UV−vis ($CHCl_3$): λ_{max} (ε, cm^{-1} M^{-1}) = 415 (360132), 527 (28597) nm; HR-FAB-MS (NBA): m/z calcd for $C_{134}H_{114}N_{14}O_4S_2Ni_2$: 2162.7296; found 2162.7346; ^{13}C NMR spectrum could not be obtained due to the low solubility.

■ ASSOCIATED CONTENT

Ⓢ Supporting Information

DFT-optimized structure, UV−vis absorption spectra, fluorescence spectra, titration data, ESI-MS spectra, NMR spectra and X-ray crystallographic data. This material is available free of charge via the Internet at http://pubs.acs.org.

■ AUTHOR INFORMATION

Corresponding Author

*E-mail: tanif@ms.ifoc.kyushu-u.ac.jp

Notes

The authors declare no competing financial interest.

■ ACKNOWLEDGMENTS

This work was supported by Grants-in-Aid (Scientific Research on Innovative Areas No. 20108009 to F.T., "pi-Space," and the Global COE Program "Science for Future Molecular Systems") from Ministry of Education, Culture, Sports, Science and Technology of Japan, by the Cooperative Research Program of Network Joint Research Center for Materials and Devices (Institute for Materials Chemistry and Engineering, Kyushu University)," and by a Research Grant to F.T. from Tokuyama Science and Technology Foundation and Iketani Science and Technology Foundation. We acknowledge Prof. T. Shinmyozu of Kyushu University for his kind cooperation on the use of GPC and microbalance instruments, Prof. H. Nakano of Kyushu University and Dr. I. Hisaki of Osaka University for their advices on DFT calculation and X-ray crystallography, respectively.

■ REFERENCES

(1) (a) Kadish, K. M.; Ruoff, R. S., Ed. *Fullerenes: Chemistry Physics and Technology*; Wiley Interscience: New York, 2000. (b) Guldi, D. M.; Martín, N., Eds.; *Fullerenes: From Synthesis to Optoelectronic Properties*; Kluwer: Dordorecht, 2002. (c) Fukuzumi, S.; Guldi, D. M. *Electron Transfer in Chemistry*; Balzani, V., Ed. Wiley-VCH: Weinheim, 2001, Vol. 2, pp 270−337. (d) Hirsch, A.; Brettreich, M. *Fullerenes: Chemistry and Reactions*; Wiley-VCH: Weinheim, 2005. (e) Langa, F., Nierengarten, J.-F., Ed. *Fullerenes: Principles and Applications*, 2nd ed; Royal Society of Chemistry Publishing: Cambridge, 2012.

(2) (a) Zhong, Z.-L.; Ikeda, A.; Shinkai, S. In *Calixarenes 2001*; Asfari, Z., Böhmer, V., Harrowfield, J., Vicens, J., Saadioui, M., Eds.; Kluwer: Dordrecht, 2001, pp 476−495. (b) Constabel, F.; Geckeler, K. E. In *Functional Nanomaterials*; Geckeler, K. E., Rosenberg, E., Eds.; American Scientific Publishers: Stevenson Ranch, 2006; pp 377−393. (c) Delgado, J. L.; Nierengarten, J.-F. In *Calixarenes in the Nanoworld*; Vicens, J., Harrowfield, J., Baklouti, L., Eds.; Springer: Dordrecht, 2007; pp 173−196. (d) Pérez, E. M.; Martín, N. *Chem. Soc. Rev.* **2008**, *37*, 1512−1519. (e) Steed, J. W.; Atwood, J. L. *Supramolecular Chemistry*, 2nd ed.; John Wiley & Sons Ltd.: Chichester, 2009. (f) Sánchez, L.; Otero, R.; Gallego, J. M.; Miranda, R.; Martín, N. *Chem. Rev.* **2009**, *109*, 2081−2091. (g) Lhoták, P.; Kundrát, O. In *Artificial Receptors for Chemical Sensors*; Mirsky, V. M., Yatsimirsky, A. K., Eds.; Wiley-VCH: Weinheim, 2011, pp 249−272. (h) Giacalone,

F.; Martín, N. *Adv. Mater.* **2010**, *22*, 4220−4248. (i) Canevet, D.; Pérez, E. M.; Martín, N. *Angew. Chem., Int. Ed.* **2011**, *50*, 9248−9259. (j) Martín, N.; Nierengarten, J.-F., Eds. *Supramolecular Chemistry of Fullerenes and Carbon Nanotubes*; Wiley-VCH: Weinheim, 2012.

(3) (a) Boyd, P. D. W.; Reed, C. A. *Acc. Chem. Res.* **2005**, *38*, 235−242. (b) Tashiro, K.; Aida, T. *Chem. Soc. Rev.* **2007**, *36*, 189−197.

(4) (a) Boyd, P. D. W.; Hodgson, M. C.; Rickard, C. E. F.; Oliver, A. G.; Chaker, L.; Brothers, P. J.; Bolskar, R. D.; Tham, F. S.; Reed, C. A. *J. Am. Chem. Soc.* **1999**, *121*, 10487−10495. (b) Sun, D.; Tham, F. S.; Reed, C. A.; Chaker, L.; Burgess, M.; Boyd, P. D. W. *J. Am. Chem. Soc.* **2000**, *122*, 10704−10705. (c) Tashiro, K.; Aida, T.; Zheng, J.-Y.; Kinbara, K.; Saigo, K.; Sakamoto, S.; Yamaguchi, K. *J. Am. Chem. Soc.* **1999**, *121*, 9477−9478. (d) Zheng, J.-Y.; Tashiro, K.; Hirabayashi, Y.; Kinbara, K.; Saigo, K.; Aida, T.; Sakamoto, S.; Yamaguchi, K. *Angew. Chem., Int. Ed.* **2001**, *40*, 1857−1861. (e) Sun, D.; Tham, F. S.; Reed, C. A.; Chaker, L.; Boyd, P. D. W. *J. Am. Chem. Soc.* **2002**, *124*, 6604−6612. (f) Ayabe, M.; Ikeda, A.; Shinkai, S.; Sakamoto, S.; Yamaguchi, K. *Chem. Commun.* **2002**, 1032−1033. (g) Yamaguchi, T.; Ishii, N.; Tashiro, K.; Aida, T. *J. Am. Chem. Soc.* **2003**, *125*, 13934−13935. (h) Shoji, Y.; Tashiro, K.; Aida, T. *J. Am. Chem. Soc.* **2004**, *126*, 6570−6571. (i) Kieran, A. L.; Pascu, S. I.; Jarrosson, T.; Sanders, J. K. M. *Chem. Commun.* **2005**, 1276−1278. (j) Hosseini, A.; Taylor, S.; Accorsi, G.; Armaroli, N.; Reed, C. A.; Boyd, P. D. W. *J. Am. Chem. Soc.* **2006**, *128*, 15903−15913. (k) Bhattacharya, S.; Tominaga, K.; Kimura, T.; Uno, H.; Komatsu, N. *Chem. Phys. Lett.* **2007**, *433*, 395−402. (l) Yanagisawa, M.; Tashiro, K.; Yamasaki, M.; Aida, T. *J. Am. Chem. Soc.* **2007**, *129*, 11912−11913. (m) Fathalla, M.; Jayawickramarajah. *J. Eur. J. Org. Chem.* **2009**, 6095−6099. (n) Gil-Ramírez, G.; Karlen, S. D.; Shundo, A.; Porfyrakis, K.; Ito, Y.; Briggs, G. A. D.; Morton, J. J. L.; Anderson, H. L. *Org. Lett.* **2010**, *12*, 3544−3547. (o) Song, J.; Aratani, N.; Shinokubo, H.; Osuka, A. *J. Am. Chem. Soc.* **2010**, *132*, 16356−16357. (p) Mulhollabd, A. R.; Woodward, C. P.; Langford, S. J. *Chem. Commun.* **2011**, *47*, 1494−1496. (q) Uno, H.; Furukawa, M.; Fujimoto, A.; Uoyama, H.; Watanabe, H.; Okujima, T.; Yamada, H.; Mori, S.; Kuramoto, M.; Iwamura, T.; Hatae, N.; Tani, F.; Komatsu, N. *J. Porphyrins Phthalocyanines* **2011**, *15*, 951−963. (r) Grimm, B.; Schornbaum, J.; Cardona, C. M.; van Paauwe, J. D.; Boyd, P. D. W.; Guldi, D. M. *Chem. Sci.* **2011**, *2*, 1530−1537. (s) Hernández-Eguía, L. P.; Escudero-Adán, E. C.; Pinzón, J. R.; Echegoyen, L.; Ballester, P. *J. Org. Chem.* **2011**, *76*, 3258−3265. (t) Hernández-Eguía, L. P.; Escudero-Adán, E. C.; Pintre, I. C.; Ventura, B.; Flamigni, L.; Ballester, P. *Chem.−Eur. J.* **2011**, *17*, 14564−14577. (u) Zhang, C.; Wang, Q.; Long, H.; Zhang, W. *J. Am. Chem. Soc.* **2011**, *133*, 20995−21001. (v) Zhang, C.; Long, H.; Zhang, W. *Chem. Commun.* **2012**, *48*, 6172−6174. (w) Sánchez-Molina, I.; Grimm, B.; Krick Calderon, R. M.; Claessens, C. G.; Guldi, D. M.; Torres, T. *J. Am. Chem. Soc.* **2013**, *135*, 10503−10511. (x) Fang, X.; Zhu, Y.-Z.; Zheng, J.-Y. *J. Org. Chem.* **2014**, *79*, 1184−1191.

(5) (a) Beletskaya, I.; Tyurin, V. S.; Tsivadze, A. Y.; Guilard, R.; Stern, C. *Chem. Rev.* **2009**, *109*, 1659−1713. (b) Drain, C. M.; Varotto, A.; Radivojevic, I. *Chem. Rev.* **2009**, *109*, 1630−1658. (c) de la Torre, G.; Bottari, G.; Sekita, M.; Hausmann, A.; Guldi, D. M.; Torres, T. *Chem. Soc. Rev.* **2013**, *42*, 8049−8105. (d) Medforth, C. J.; Wang, Z.; Martin, K. E.; Song, Y.; Jacobsen, J. L.; Shelnutt, J. A. *Chem. Commun.* **2009**, 7261−7277. (e) Chambron, J.-C.; Heitz, V.; Sauvage, J.-P. In *The Porphyrin Handbook*; Kadish, K. M., Smith, K. M., Guilard, R., Eds.; Academic Press: San Diego, 2000; Vol. *6*, pp 1−42.

(6) (a) Gust, D.; Moore, T. A. In *The Porphyrin Handbook*; Kadish, K. M., Smith, K. M., Guilard, R., Eds.; Academic Press: San Diego, 2000; Vol. *8*, pp 153−190. (b) Kadish, K. M., Smith, K. M., Guilard, R., Eds. *Handbook of Porphyrin Science*; World Scientific, Singapore, 2010. (c) Gust, D.; Moore, T. A.; Moore, A. L. *Acc. Chem. Res.* **2001**, *34*, 40−48. (d) Fukuzumi, S. *Org. Biomol. Chem.* **2003**, *1*, 609−620. (e) El-Khouly, M. E.; Ito, O.; Smith, P. M.; D'Souza, F. *J. Photochem. Photobiol. C* **2004**, *5*, 79−104. (f) Guldi, D. M.; Rahman, G. M. A.; Zerbetto, F.; Prato, M. *Acc. Chem. Res.* **2005**, *38*, 871−878. (g) Guldi, D. M. *Phys. Chem. Chem. Phys.* **2007**, *9*, 1400−1420. (h) Fukuzumi, S. *Phys. Chem. Chem. Phys.* **2008**, *10*, 2283−2297. (i) Gust, D.; Moore, T. A.; Moore, A. *Acc. Chem. Res.* **2009**, *42*, 1890−1898. (j) Hasobe, T. *Phys. Chem. Chem. Phys.* **2010**, *12*, 44−57. (k) D' Souza, F.; Sandanayaka, A. S. D.; Ito, O. *J. Phys. Chem. Lett.* **2010**, *1*, 2586−2593. (l) Fukuzumi, S.; Ohkubo, K. *J. Mater. Chem.* **2012**, *22*, 4575−4587. (m) Hasobe, T. *J. Phys. Chem. Lett.* **2013**, *4*, 1771−1780.

(7) (a) Guldi, D. M. *Chem. Soc. Rev.* **2002**, *31*, 22−36. (b) Imahori, H.; Mori, Y.; Matano, Y. *J. Photochem. Photobiol. C* **2003**, *4*, 51−83. (c) D'Souza, F.; Ito, O. *Coord. Chem. Rev.* **2005**, *249*, 1410−1422. (d) Fukuzumi, S. *Bull. Chem. Soc. Jpn.* **2006**, *79*, 177−195. (e) Imahori, H. *Bull. Chem. Soc. Jpn.* **2007**, *80*, 621−636. (f) Fukuzumi, S.; Kojima, T. *J. Mater. Chem.* **2008**, *18*, 1427−1439. (g) D'Souza, F.; Ito, O. *Chem. Commun.* **2009**, 4913−4928. (h) Fukuzumi, S.; Honda, T.; Ohkubo, K.; Kojima, T. *Dalton Trans.* **2009**, 3880−3889. (i) Wasielewski, M. R. *Acc. Chem. Res.* **2009**, *42*, 1910−1921. (j) Ohkubo, K.; Fukuzumi, S. *Bull. Chem. Soc. Jpn.* **2009**, *82*, 303−315. (k) Bottari, G.; de la Torre, G.; Guldi, D. M.; Torres, T. *Chem. Rev.* **2010**, *110*, 6768−6816. (l) D'Souza, F.; Ito, O. *Chem. Soc. Rev.* **2012**, *41*, 86−96. (m) Imahori, H.; Umeyama, T.; Kurotobi, K.; Takano, Y. *Chem. Commun.* **2012**, *48*, 4032−4045. (n) Gust, D.; Moore, T. A.; Moore, A. L. *Faraday Discuss.* **2012**, *155*, 9−26. (o) Bottari, G.; Trukhina, O.; Ince, M.; Torres, T. *Coord. Chem. Rev.* **2012**, *256*, 2453−2477. (p) Ito, O.; D'Souza, F. *Molecules* **2012**, *17*, 5816−5835. (q) Schuster, D. I. *J. Org. Chem.* **2013**, *78*, 6811−6841. (r) Fukuzumi, S.; Ohkubo, K. *Dalton Trans.* **2013**, *42*, 15846−15858. (s) Yoosaf, K.; Iehl, J.; Nierengarten, I.; Hmadeh, M.; Albrecht-Gary, A.-M.; Nierengarten, J.-F.; Armaroli, N. *Chem. −Eur. J.* **2014**, *20*, 223−231.

(8) (a) Imahori, H.; Guldi, D. M.; Tamaki, K.; Yoshida, Y.; Luo, C.; Sakata, Y.; Fukuzumi, S. *J. Am. Chem. Soc.* **2001**, *123*, 6617−6628. (b) Fukuzumi, S.; Ohkubo, K.; Imahori, H.; Shao, J.; Ou, Z.; Zheng, G.; Chen, Y.; Pandey, R. K.; Fujitsuka, M.; Ito, O.; Kadish, K. M. *J. Am. Chem. Soc.* **2001**, *123*, 10676−10683. (c) Imahori, H.; Sekiguchi, Y.; Kashiwagi, Y.; Sato, T.; Araki, Y.; Ito, O.; Yamada, H.; Fukuzumi, S. *Chem.−Eur. J.* **2004**, *10*, 3184−3196. (d) Ohkubo, K.; Kotani, H.; Shao, J.; Ou, Z.; Kadish, K. M.; Li, G.; Pandey, R. K.; Fujitsuka, M.; Ito, O.; Imahori, H.; Fukuzumi, S. *Angew. Chem., Int. Ed.* **2004**, *43*, 853−856.

(9) (a) Imahori, H.; Fukuzumi, S. *Adv. Funct. Mater.* **2004**, *14*, 525−536. (b) Martín, N.; Sánchez, L.; Herranz, M. A.; Illescas, B.; Guldi, D. M. *Acc. Chem. Res.* **2007**, *40*, 1015−1024. (c) Günes, S.; Neugebauer, H.; Sariciftci, N. S. *Chem. Rev.* **2007**, *107*, 1324−1338. (d) Kamat, P. V. *J. Phys. Chem. C* **2007**, *111*, 2834−2860. (e) Thompson, B. C.; Fréchet, J. M. J. *Angew. Chem., Int. Ed.* **2008**, *47*, 58−77. (f) Dennler, G.; Scharber, M. C.; Brabec, C. J. *Adv. Mater.* **2009**, *21*, 1323−1338. (g) Imahori, H.; Umeyama, T.; Ito, S. *Acc. Chem. Res.* **2009**, *42*, 1809−1818. (h) Guldi, D. M.; Illescas, B. M.; Atienza, C. M.; Wielopolski, M.; Martín, N. *Chem. Soc. Rev.* **2009**, *38*, 1587−1597. (i) Martínez-Díaz, M. V.; de la Torre, G.; Torres, T. *Chem. Commun.* **2010**, *46*, 7090−7108. (j) Delgado, J. L.; Bouit, P.-A.; Filippone, S.; Herranz, M. A.; Martín, N. *Chem. Commun.* **2010**, *46*, 4853−4865.

(10) (a) Kira, A.; Umeyama, T.; Matano, Y.; Yoshida, K.; Isoda, S.; Park, J. K.; Kim, D.; Imahori, H. *J. Am. Chem. Soc.* **2009**, *131*, 3198−3200. (b) Matsuo, Y.; Sato, Y.; Niinomi, T.; Soga, I.; Tanaka, H.; Nakamura, E. *J. Am. Chem. Soc.* **2009**, *131*, 16048−16050. (c) Moon, J. S.; Lee, J. K.; Cho, S.; Byun, J.; Heeger, A. J. *Nano Lett.* **2009**, *9*, 230−234. (d) Hoppe, H.; Sariciftci, N. S. *J. Mater. Chem.* **2006**, *16*, 45−61. (e) Hoppe, H.; Niggemann, M.; Winder, C.; Kraut, J.; Hiesgen, R.; Hinsch, A.; Meissner, D.; Sariciftci, N. S. *Adv. Funct. Mater.* **2004**, *14*, 1005−1011.

(11) Pasini, D.; Ricci, M. *Curr. Org. Synth.* **2007**, *4*, 59−80.

(12) (a) Nobukuni, H.; Shimazaki, Y.; Tani, F.; Naruta, Y. *Angew. Chem., Int. Ed.* **2007**, *46*, 8975−8978. (b) Nobukuni, H.; Tani, F.; Shimazaki, Y.; Naruta, Y.; Ohkubo, K.; Nakanishi, T.; Kojima, T.; Fukuzumi, S.; Seki, S. *J. Phys. Chem. C* **2009**, *113*, 19694−19699. (c) Nobukuni, H.; Shimazaki, Y.; Uno, H.; Naruta, Y.; Ohkubo, K.; Kojima, T.; Fukuzumi, S.; Seki, S.; Sakai, H.; Hasobe, T.; Tani, F. *Chem.−Eur. J.* **2010**, *16*, 11611−11623. (d) Nobukuni, H.; Kamimura, T.; Uno, H.; Shimazaki, Y.; Naruta, Y.; Tani, F. *Bull. Chem. Soc. Jpn.* **2011**, *84*, 1321−1328. (e) Nobukuni, H.; Kamimura, T.; Uno, H.; Shimazaki, Y.; Naruta, Y.; Tani, F. *Bull. Chem. Soc. Jpn.* **2012**, *85*, 869−

876. (f) Kamimura, T.; Ohkubo, K.; Kawashima, Y.; Nobukuni, H.; Naruta, Y.; Tani, F.; Fukuzumi, S. *Chem. Sci.* **2013**, *4*, 1451−1461.
(13) Guldi, D. M.; Hungerbühler, H.; Carmichael, I.; Asmus, K. −D.; Maggini, M. *J. Phys. Chem. A* **2000**, *104*, 8601−8608.
(14) Though the zigzag array of C_{60} as observed in the crystal of C_{60}⊂H_4-C_4-CPD_{Py}(H) is attractive itself, it is rather difficult to design a host molecule for a zigzag array of fullerenes because such array is induced mainly by van del Waals interaction of fullerenes instead of self-assembly of a host molecule. The design of a host molecule for a self-assembled nanotube structure is more rational and straightforward. This is the reason why we have chosen self-assembled nanotube structure for the control of fullerene arrangement.
(15) (a) Rosokha, S. V.; Kochi, J. K. *J. Am. Chem. Soc.* **2007**, *129*, 3683−3697. (b) Krämer, C. S.; Zeitler, K.; Müller, T. J. J. *Org. Lett.* **2000**, *2*, 3723−3726. (c) Krämer, C. S.; Müller, T. J. J. *Eur. J. Org. Chem.* **2003**, *18*, 3534−3548. (d) Wang, H.; Xu, W.; Zhang, B. *J. Chem. Crystallogr.* **2012**, *42*, 846−850. (e) Li, D.; Tian, X.; Hu, G.; Zhang, Q.; Wang, P.; Sun, P.; Zhou, H.; Meng, X.; Yang, J.; Wu, J.; Jin, B.; Zhang, S.; Tao, X.; Tian, Y. *Inorg. Chem.* **2011**, *50*, 7997−8006.
(16) Frisch, M. J.; Trucks, G. W.; Schlegel, H. B.; Scuseria, G. E.; Robb, M. A.; Cheeseman, J. R.; Scalmani, G.; Barone, V.; Mennucci, B.; Petersson, G. A.; Nakatsuji, H.; Caricato, M.; Li, X.; Hratchian, H. P.; Izmaylov, A. F.; Bloino, J.; Zheng, G.; Sonnenberg, J. L.; Hada, M.; Ehara, M.; Toyota, K.; Fukuda, R.; Hasegawa, J.; Ishida, M.; Nakajima, T.; Honda, Y.; Kitao, O.; Nakai, H.; Vreven, T.; Montgomery, J. A., Jr.; Peralta, J. E.; Ogliaro, F.; Bearpark, M.; Heyd, J. J.; Brothers, E.; Kudin, K. N.; Staroverov, V. N.; Keith, T.; Kobayashi, R.; Normand, J.; Raghavachari, K.; Rendell, A.; Burant, J. C.; Iyengar, S. S.; Tomasi, J.; Cossi, M.; Rega, N.; Millam, J. M.; Klene, M.; Knox, J. E.; Cross, J. B.; Bakken, V.; Adamo, C.; Jaramillo, J.; Gomperts, R.; Stratmann, R. E.; Yazyev, O.; Austin, A. J.; Cammi, R.; Pomelli, C.; Ochterski, J. W.; Martin, R. L.; Morokuma, K.; Zakrzewski, V. G.; Voth, G. A.; Salvador, P.; Dannenberg, J. J.; Dapprich, S.; Daniels, A. D.; Farkas, Ö.; Foresman, J. B.; Ortiz, J. V.; Cioslowski, J.; Fox, D. J. *Gaussian 09*, Revision D.01; Gaussian, Inc.: Wallingford CT, 2013.
(17) Huang, W.; Wang, M.; Du, C.; Chen, Y.; Qin, R.; Su, L.; Zhang, C.; Liu, Z.; Li, C.; Bo, Z. *Chem. −Eur. J.* **2011**, *17*, 440−444.
(18) Ruzié, C.; Michaudet, L.; Boitrel, B. *Tetrahedron Lett.* **2002**, *43*, 7423−7426.
(19) The yields of the monomer porphyrins are relatively low in comparison with typical tetraphenylporphyrins (∼30%). Although the reaction conditions have not been thoroughly optimized, possible reasons are the low solubility and strong affinity to silica gel of the pyridyl-substituted porphyrins. In fact, they showed substantial tailing during the silica gel column chromatography. Scrambling of the *meso*-substituents was not observed in the products.
(20) Lin, H. H.; Chang, C. C. *Dyes Pigments* **2009**, *83*, 230−236.
(21) (a) Armaroli, N.; Diederich, F.; Echegoyen, L.; Habicher, T.; Flamigni, L.; Marconi, G.; Nierengarten, J. −F. *New. J. Chem.* **1999**, *23*, 77−83. (b) Elhabiri, M.; Trabolsi, A.; Cardinali, F.; Hahn, U.; Albrecht-Gary, A. −M.; Nierengarten, J. −F. *Chem. −Eur. J.* **2005**, *11*, 4793−4798.
(22) On the basis of a number of previous X-ray crystallographic analyses of low-spin four-coordinate Ni(II) porphyrins showing ruffled distortions, the two nickel porphyrin moieties in C_{60}⊂Ni_2-Ptz-CPD_{Py}(OC_6) should have the same distortions, although we have not clarified its detailed structure. See reviews and references cited therein: (a) Sheidt, W. R. In *The Porphyrin Handbook*; Kadish, K. M., Smith, K. M., Guilard, R., Eds.; Academic Press: San Diego, 2000; Vol. 3, pp 49−112. (b) Sheidt, W. R. In *Handbook of Porphyrin Science*; Kadish, K. M., Smith, K. M., Guilard, R., Eds.; World Scientific: Singapore, 2012; Vol. *24*, pp 1−179.
(23) (a) David, W. I. F.; Ibberson, R. M.; Matthewman, J. C.; Prassides, K.; Dennis, T. J. S.; Hare, J. P.; Kroto, H. W.; Taylor, R.; Walton, D. R. M. *Nature* **1991**, *353*, 147−149. (b) McKenzie, D. R.; Davis, C. A.; Cockayne, D. J. H.; Muller, D. A.; Vassallo, A. M. *Nature* **1992**, *353*, 622−624. (c) Nikolaev, A. V.; Dennis, T. J. S.; Prassides, K.; Soper, A. K. *Chem. Phys. Lett.* **1994**, *223*, 143−148. (d) van Smaalen, S.; Petricek, V.; de Boer, J. L.; Dusek, M.; Verheijen, M. A.; Meijer, G. *Chem. Phys. Lett.* **1994**, *223*, 323−328.
(24) Ouchi, A.; Tashiro, K.; Yamaguchi, K.; Tsuchiya, T.; Akasaka, T.; Aida, T. *Angew. Chem., Int. Ed.* **2006**, *45*, 3542−3546.
(25) The distance between the inside *ortho* hydrogen atoms of the opposite phenyl rings: 8.318(1) Å for C_{60}⊂Ni_2-C_4-CPD_{Py}(H) and 10.20(1) Å for C_{60}⊂H_4-Ptz-CPD_{Py}(OC_3). In the case of C_{60}⊂Ni_2-C_4-CPD_{Py}(H), the four inside *ortho* C−H moieties of the phenyl rings prevent the center location of C_{60}.
(26) Burla, M. C.; Caliandro, R.; Camalli, M.; Carrozzini, B.; Cascarano, G. L.; Caro, L. D.; Giacovazzo, C.; Polidori, G.; Spagna, R. *J. Appl. Crystallogr.* **2005**, *38*, 381−388.
(27) Crystal Structure Analysis Software, *Crystal Structure* 4.0; Rigaku Corporation: Tokyo, Japan, 2010.
(28) (a) Programs for the solution and the refinement of the crystal structure from diffraction data, *SHELX97* and *SHELXL-97*, respectively, University of Göttingen: Göttingen, Germany. (b) Sheldrick, G. M. *Acta Crystallogr., Sect. A* **2008**, *64*, 112−122.
(29) *PLATON*, A Multipurpose Crystallographic Tool: Spek, A. L. *J. Appl. Crystallogr.* **2003**, *36*, 7−13.
(30) Lin, C.-H.; Tour, J. *J. Org. Chem.* **2002**, *67*, 7761−7768.